BAINITIC TRANSFORMATION IN LOW CARBON MICRO-ALLOYED HOT FORGED STEELS FOR DIESEL ENGINE COMPONENTS

A THESIS SUBMITTED TO
THE GRADUATE SCHOOL OF NATURAL AND APPLIED SCIENCES
OF
MIDDLE EAST TECHNICAL UNIVERSITY

BY

BURAK KESKIN

IN PARTIAL FULFILLMENT OF THE REQUIREMENTS
FOR
THE DEGREE OF MASTER OF SCIENCE
IN
METALLURGICAL AND MATERIALS ENGINEERING

DECEMBER 2019

Approval of the thesis:

BAINITIC TRANSFORMATION IN LOW CARBON MICRO-ALLOYED HOT FORGED STEELS FOR DIESEL ENGINE COMPONENTS

submitted by **BURAK KESKIN** in partial fulfillment of the requirements for the degree of **Master of Science in Metallurgical and Materials Engineering Department, Middle East Technical University** by,

Prof. Dr. Halil Kalıpçılar
Dean, Graduate School of **Natural and Applied Sciences** _____

Prof. Dr. Hakan Gür
Head of Department, **Met. and Mat. Eng.** _____

Prof. Dr. Bilgehan Ögel
Supervisor, **Met. and Mat. Eng., METU** _____

Examining Committee Members:

Prof. Dr. Ali Kalkanlı
Met. and Mat. Eng., METU _____

Prof. Dr. Bilgehan Ögel
Met. and Mat. Eng., METU _____

Assist. Prof. Dr. Batur Ercan
Met. and Mat. Eng., METU _____

Prof. Dr. Nuri Durlu
Met. and Mat. Eng., TOBB ETU _____

Assist. Prof. Dr. Bilge İmer
Met. and Mat. Eng., METU _____

Date: 06.12.2019

I hereby declare that all information in this document has been obtained and presented in accordance with academic rules and ethical conduct. I also declare that, as required by these rules and conduct, I have fully cited and referenced all material and results that are not original to this work.

Name, Surname: Burak Keskin

Signature:

ABSTRACT

BAINITIC TRANSFORMATION IN LOW CARBON MICRO-ALLOYED HOT FORGED STEELS FOR DIESEL ENGINE COMPONENTS

Keskin, Burak
Master of Science, Metallurgical and Materials Engineering
Supervisor: Prof. Dr. Bilgehan Ögel

December 2019, 86 pages

In recent years, the fuel injection pressures increased to very high level for more efficient internal combustion engines. With developing technology, it is expected that components must resist at least 2500 bar pressure working conditions. These high pressure levels must accompany with better properties such as mechanical, fatigue and corrosion. Automotive industry mostly use quenched and tempered steels for such critical applications. However, it is known that, bainitic steels have better mechanical properties in terms of UTS, toughness and fatigue. In recent years, bainitic forging steels are emerged as an alternative to Q&T steels. Furthermore, as bainite forms during continuous cooling from austenite region, the Q&T steps is omitted. However, there are only a few bainitic forging grade steels in the market. In this study, the bainite formation and its effect on mechanical properties of a continuous cooled forging grade experimental steel is investigated. By using the calculated CCT diagrams (Continuous Cooling Transformation), a basic alloy 0.2C-1.50Si-1.40Mn-1.45(Cr+Mo) is selected as an experimental steel. The formation of bainite and its morphology upon different cooling rates is observed. The effect of Ti, Nb and S addition on properties is also studied. The amount of retained austenite of the samples are analyzed using XRD. The DTA analysis is used to find the exact B_s and M_s temperature of the steel. The tensile strength and charpy impact toughness tests are carried out. It is found that the 0.01%Ti

added experimental steel yields high toughness levels (around 20J) at a strength level of 1250 MPa and 16% elongation. Furthermore, it is found that the bainite formation is possible at a large interval of cooling rate which can be an advantage in industrial forging practice.

Keywords: Steel, Bainite, Retained Austenite, Bainitic Forging Steel, Continuous Cooling, Mechanical Properties, New Alloy Design in Bainitic Microstructure

ÖZ

SICAK DÖVÜLMÜŞ DİZEL MOTOR PARÇALARI İÇİN KULLANILAN DÜŞÜK KARBONLU MİKRO ALAŞIMLI ÇELİKLERİN BEYNİTİK DÖNÜŞÜMLERİ

Keskin, Burak
Yüksek Lisans, Metalurji ve Malzeme Mühendisliği
Tez Danışmanı: Prof. Dr. Bilgehan Ögel

Aralık 2019, 86 sayfa

İçten yanmalı motorlarda yüksek verimin sağlanabilmesi için istenilen basınç seviyeleri gün geçtikçe artmaktadır. Gelişen teknolojiyle birlikte, motorun içindeki parçaların en az 2500 barlık basınçtaki çalışma koşullarına dayanıklı olması gerekmektedir. Bu yüksek basınç seviyeleri, kullanılan parçaların mekanik, yorulma ve korozyon özelliklerindeki gereklilikleri de beraberinde arttırmaktadır. Otomotiv endüstrisi motorda kritik parçalar için genellikle ıslah çelikleri kullanmaktadır. Ancak, beynitik çeliklerin daha yüksek çekme dayancı, tokluk, yorulma sağlayabildiği bilinmektedir. Son yıllarda beynitik dövmelik çelikler ıslah çeliklerine alternatif olarak ortaya çıkmıştır. Üstelik östenit bölgesinden sürekli soğuma ile çelikte beynit elde edilebilirse, beynit oluşumu için izotermal ısıl işlem proseslerine gerek kalmamaktadır. Ancak piyasadaki beynitik dövmelik çelik sayısı fazla değildir. Bu çalışmada, sürekli soğuma prosesinden geçmiş deneysel dövmelik çelik kalitelerinde beynit oluşumu ve beynitin mekanik özelliklere etkisi incelenir. Hesaplanmış sürekli soğuma dönüşüm eğrileri kullanılarak 0.2C-1.50Si-1.40Mn-1.45(Cr+Mo) alaşımlı çeliği deneysel çelik olarak seçilmiştir. Farklı soğuma hızlarında beynit oluşumu ve oluşan beynitin morfolojisi gözlemlenir. Ayrıca, Ti, Nb ve S miktarının çeliğin özellikleri üzerindeki etkisi de çalışılmıştır. Deneysel

kalitelerin kalıntı östenit miktarı X-ışınları kırınımı ile analiz edilmiştir. Çeliğin kesin M_s ve B_s sıcaklık dereceleri tayini için diferansiyel termal analiz (DTA) metodları kullanılmıştır. Deneysel çeliklere çekme dayanımı ve çentik darbe dayanımı testleri uygulanmıştır. %0,01 oranında Ti eklenmiş deneysel çeliğin 1250Mpa çekme dayancı ve %16 uzama gösterirken aynı zamanda yüksek tokluk seviyeleri (yaklaşık 20J) de gösterdiği görülmüştür. Buna ek olarak, beynit daha geniş soğuma hızı aralığında oluşmaktadır. Bu durum çeliğin endüstriyel dövme uygulamalarında daha geniş bir yelpazede kullanımına olanak sağlar.

Anahtar Kelimeler: Çelik, Beynit, Kalıntı Östenit, Beynitik Dövme Çelik, Sürekli Soğutma, Mekanik Özellikler, Beynitik Mikroyapıda Yeni Alaşım Tasarımı

To my lovely wife…

ACKNOWLEDGEMENTS

Foremost, I would like to express my sincerest gratitude and thanks to my supervisor Prof. Dr. Bilgehan ÖGEL for the continuous support throughout this study. He guided with his valuable comments, support, understanding and patience. I could not imagined having a better advisor and mentor for this work.

I would like to thank ÇEMTAŞ A.Ş. for their financial support and my managers İ.İrfan AYHAN, İbrahim GÖKÇE and Berkay ŞAHİN for their guidance, experiences and help during this study. Also I would like to express my gratitude R&D Department in ÇEMTAŞ A.Ş. Without their support, I could not have been successfully conducted all my experiments. Special thanks to Caner GÜNEY, Bertan PARMAKSIZOĞLU, N. Başak DÜRGER, Emre ALAN and Suat ŞENOL for their help and technical assistance through this entire study.

I am indebted to my parents, Vesile KESKİN, Mustafa KESKİN and my sister Sezen AYBEY for supporting me with their caring, inspiration, understanding, love, guidance and wisdom through my entire life.

My sincere thanks also goes to my friends, Osman Emre UZER, Deniz ACET and Mert KOÇER for their endless support and encourage during this research. I have been blessed with their cheerful friendship and fun in last three years.

I also owes my deepest gratitude to my love, Elvan BULUT for her great love, encouragement and motivation. Not only my thesis but also my life get easier with your endless support and patience. I really appreciate your existence.

TABLE OF CONTENTS

ABSTRACT v

ÖZ vii

ACKNOWLEDGEMENTS x

TABLE OF CONTENTS xi

LIST OF TABLES xiv

LIST OF FIGURES xv

LIST OF ABBREVIATIONS AND SYMBOLS xviii

1. INTRODUCTION 1

2. THEORY 3

2.1. Bainite 3

2.1.1. Bainite Transformation 4

2.1.2. Bainite morphology 7

2.1.3. Stability of retained austenite 9

2.1.4. Bainite classification 11

2.1.5. Mechanical Properties of Bainite 14

2.1.6. The effect of alloying elements 15

2.1.6.1. Carbon 16

2.1.6.2. Manganese 17

2.1.6.3. Silicon 18

2.1.6.4. Chromium 18

2.1.6.5. Molybdenum 19

2.1.6.6. Titanium, Aluminum, Niobium and Vanadium 19

2.1.6.7. Boron 20
2.1.7. The effect of process 21
2.1.8. The Effect of Austenitic Grain Size on Bainite Transformation 22
2.1.9. Bainitic Forging Steels 25
2.1.9.1. Chemical Compositions of Bainitic Forging Steels 25
2.1.9.2. Production of Bainitic Forging Steels 26
3. EXPERIMENTAL PROCEDURE 29
3.1. Chemical Composition 29
3.1.1. CCT diagrams 31
3.2. Production 31
3.3. Sample Preparation 33
3.3.1. Samples for mechanical tests 33
3.3.2. Metallography samples 34
3.3.3. Dilatometer samples 34
3.3.4. X-ray diffraction samples 35
4. EXPERIMENTAL RESULTS 37
4.1. Alloy composition design 37
4.2. Metallographic Examinations 38
4.2.1. Optical microscope images 38
4.2.2. SEM images 43
4.2.3. Austenite grain size results 54
4.3. Mechanical Properties 55
4.4. Dilatometer Results 59
4.5. XRD Results 71

5. DISCUSSION.....75
5.1. Alloying elements.....75
5.2. Mechanical Properties.....76
5.3. Metallographic examinations.....77
5.4. CCT diagrams.....77
5.5. X-Ray Diffraction.....77
6. CONCLUSION.....79
REFERENCES.....81

LIST OF TABLES

TABLES

Table 2-1Mechanical properties of AISI 1095 steel at room temperature with different heat treatments 15
Table 2-2 Effects of bainite transformation time on tensile strength, elongation and amount of retained austenite [43] 22
Table 2-3 Effects of austenitizing temperature [44] 24
Table 2-4 Chemical compositions of different bainitic forging steel grades [45] 26
Table 3-1 Determined chemical composition of new alloys 29
Table 3-2 Number of cast for each grades 30
Table 4-1 Bainite thickness results 53
Table 4-2 Tensile ductility comparison of each grade 58
Table 4-3 Volume fraction of retained austenite of each grade 74

LIST OF FIGURES

FIGURES

Figure 2-1 Microstructure visions of eutectoid steel a. Pearlite formation at 720oC b. Bainite obtained with isothermal transformation at 290oC c. Bainite obtained with isothermal transformation at 180oC d. Martensite [4] 4
Figure 2-2 TTT diagram of eutectoid steel (γ: Austenite, Ms: Martensite start)[6] 5
Figure 2-3 Bainite under Scanning Electron Microscope [7] 5
Figure 2-4 Lateral growth of bainite structure [9] 6
Figure 2-5 Bulky and thin film structure of retained austenite in bainite morphology [9] 9
Figure 2-6 Transformation of upper and lower bainite schematically [4] 12
Figure 2-7 Microstructure of upper and lower bainite schematically [28] 13
Figure 2-8 According to Spanos and others, bainite classes in different carbon content and temperature [9] 14
Figure 2-9 Austenite and ferrite stabilizer alloying elements and their effects in terms of ΔH [9] 16
Figure 2-10 T_0 is shown in terms of carbon concentration and free energy for ferrite/austenite phase transformation [30] 17
Figure 2-11 Cementite formation temperatures with different amount of Silicon content [34] 18
Figure 2-12 SEM image of TiN inclusion [34] 19
Figure 2-13 Effect of micro-alloying elements on austenitic grain size [38] 20
Figure 2-14 Retained austenite amount in terms of time and temperature [42] 21
Figure 2-15 Effect of austenite grain size on bainite morphology [4] 23
Figure 2-16 Microstructure images of samples austenitized for 20 minutes at different temperatures [44] 24

Figure 2-17 Applied heat treatments for Q&T steels and bainitic steels after forging 27
Figure 3-1 Induction furnace 31
Figure 3-2 Vacuum tank 31
Figure 3-3 80x80x110mm mould 32
Figure 3-4 Mould heater 32
Figure 3-5 Sample shaping with forging and machining processes 33
Figure 3-6 Tensile test sample dimensions 34
Figure 3-7 Dilatometer sample 35
Figure 4-1 CCT diagram output from JmatPro 37
Figure 4-2 G1 vs Reference steel grade under optical microscope 39
Figure 4-3 G4 vs Reference steel grade under optical microscope 39
Figure 4-4 G5 vs Reference steel grade under optical microscope 40
Figure 4-5 G6 vs Reference steel grade under optical microscope 40
Figure 4-6 G1 vs Reference steel grade under optical microscope 41
Figure 4-7 G4 vs Reference steel grade under optical microscope 41
Figure 4-8 G5 vs Reference steel grade under optical microscope 42
Figure 4-9 G6 vs Reference steel grade under optical microscope 42
Figure 4-10 SEM micrographs of reference steel grade after hot forging and continuous cooling **a.** 1000x magnification **b.** 3000x magnification **c.** 5000x magnification 43
Figure 4-11 SEM micrographs of G1 after hot forging and continuous cooling **a.** 1000x magnification **b.** 3000x magnification **c.** 5000x magnification 45
Figure 4-12 SEM micrographs of G4 after hot forging and continuous cooling **a.** 1000x magnification **b.** 3000x magnification **c.** 5000x magnification 47
Figure 4-13 SEM micrographs of G5 after hot forging and continuous cooling **a.** 1000x magnification **b.** 3000x magnification **c.** 5000x magnification 49
Figure 4-14 SEM micrographs of G6 after hot forging and continuous cooling **a.** 1000x magnification **b.** 3000x magnification **c.** 5000x magnification 51

Figure 4-15 Bainitic ferrite between flat type of M/A phase under SEM, 20000x magnification.....53
Figure 4-16 Austenite grain size of each steel grade according to ASTM E-112.....54
Figure 4-17 Yield strength comparison of each steel grade.....55
Figure 4-18 Tensile strength comparison of each steel grade.....55
Figure 4-19 Elongation percent comparison of each steel grade 56
Figure 4-20 Reduction area percent comparison of each steel grade.....56
Figure 4-21 Toughness comparison of each steel grade 57
Figure 4-22 Hardness comparison of each steel grade.....57
Figure 4-23 Precise CCT diagram of reference steel grade with hardness values in different cooling rates 59
Figure 4-24 Microstructure images of reference steel grade with different cooling rates **a.**42K/sec **b.**30K/sec **c.**16K/sec **d.**8K/sec **e.**2K/sec **f.**1K/sec **g.**0,5K/sec **h.**0,3K/sec **i.**0,15K/sec 60
Figure 4-25 Precise CCT diagram of G4 with hardness values in different cooling rates 65
Figure 4-26 Microstructure images of G4 with different cooling rates **a.** 42K/sec **b.** 30K/sec **c.**16K/sec **d.**8K/sec **e.**2K/sec **f.**1K/sec **g.**0,5K/sec **h.**0,3K/sec **i.**0,15K/sec .66
Figure 4-27 Diffraction angles of Reference Steel Grade by using Cu-K α radiation 71
Figure 4-28 Diffraction angles of G1 by using Cu-K α radiation.....72
Figure 4-29 Diffraction angles of G4 by using Cu-K α radiation.....72
Figure 4-30 Diffraction angles of G5 by using Cu-K α radiation.....73
Figure 4-31 Diffraction angles of G6 by using Cu-K α radiation.....73

LIST OF ABBREVIATIONS AND SYMBOLS

α : Ferrite

μm : Micrometer

γ : Austenite

σt : Tensile Strength

σy : Yield Strength

δ : Elongation

d : Diameter

Ac_1 : Temperature (^oC) that austenite formation start during heated up

Ac_3 : Temperature (^oC) that ferrite completely transforms austenite during heated up

AFP : Age hardening ferritic pearlitic

AISI : American Iron and Steel Institute

Al : Aluminum

AlN : Aluminum nitride

ASTM : American Society for Testing Materials

B : Boron

B_2O_3 : Boron oxide

BN : Boron nitride

B_s : Bainite formation start temperature

C : Carbon

Ca : Calcium

CCT : Continuous Cooling Transformation

Cr : Chromium

Cu : Copper

Fe : Iron

$Fe_{2,4}C$: ε-Carbide

Fe_3C : Cementite

GPa : Gigapascal

HB	: Hardness in terms of Brinell
HR_C	: Hardness in terms of Rockwell C
HV	: Hardness in terms of Vickers
ΔH	: Enthalpy change
J	: Joule
K	: Kelvin
mm	: Millimeter
Mn	: Manganese
Mo	: Molybdenum
M/A	: Martensite / Austenite
MPa	: Megapascal
M_s	: Martemsite formation start temperature
N	: Nitrogen
Nb	: Niobium
Ni	: Nickel
Q&T	: Quenched and Tempered
S	: Sulphur
sec	: Second
SEM	: Scanning Electron Microscope
Si	: Silicon
Sn	: Tin
P	: Phosphorus
T	: Temperature
T_0	: Temperature that required for bainitic transformation
t	: time
TTT	: Time-Temperature-Transformation
Ti	: Titanium
TiN	: Titanium nitride
Ti(C, N)	: Titanium carbonitride
TRIP	: Transformation Induced Plasticity

CHAPTER 1

INTRODUCTION

Automotive industry mostly use forging steels as ferritic-pearlitic or quenched and tempered steels. By adding micro-alloying elements during steelmaking processes, the strength of ferritic pearlitic steels can be enhanced. Those have significant effect on refining the grain size. Micro-alloyed ferritic pearlitic steels are preferred since heat treatment steps are omitted. However, ferritic pearlitic steels indicate inferior values of toughness and yield strength in comparison to quenched and tempered steels. Thus, bainitic steels step in with higher toughness while maintaining high strength and hardness values. Bainite microstructure can be obtained by isothermal heat treatment but it is a long and costly process which limits industrial application.

For example, considering a common-rail diesel injector with a pressure of up to 3000 bar, these requirements are high tensile strength, excellent fatigue behaviour, acceptable weldability and good machinability [1]. The high strength values also provide high fatigue limits.

In recent years, bainitic forging steels are emerged as an alternative to Q&T steels [2, 3]. By using the calculated CCT diagrams (Continuous Cooling Temperature) and by adjusting the alloying element content precisely, the ferrite and pearlite transformation can be retarded but bainite formation enhanced. In these steels, the bainite transformation becomes possible under continuous cooling from austenite region, because the bainitic transformation is encouraged due to suppression of ferrite and pearlite. However, there are only a few bainitic forging grade steels in the market and considerable research is going on these steels to further improve their toughness and strength values [3].

This study focuses on a new grade of forging quality steel with bainitic microstructure. It is aimed to obtain a bainitic structure upon continuous cooling process after forging. The alloying element additions are aimed to obtain a carbide free bainitic structure at a lower carbon content than the commercially available competitive steels, which might improve the toughness of the steel. The hardenability of the new steel should be enough to avoid formation of any ferrite and pearlite as well.

The influences of micro-alloying elements are investigated by designing different content of titanium and niobium to decide most convenient material during this work.

CHAPTER 2

THEORY

2.1. Bainite

Until the end of 1920s, fine pearlite and martensite transformation is known when the phase transformations are started to investigate by heat treatments. In 1930, Davenport and Bain found out different and intrinsic morphology between martensite and pearlite transformation temperatures under optical microscope. They found out in that temperature range the microstructure has different morphology when it is both compared with pearlite and martensite. First, this morphology is called “acicular dark aggregate” and seemed similar with carbide precipitation in tempered martensite it is also called “martensite-troostie”. During researches, this new morphology gave better toughness values than martensite and also showed promising mechanical values. In 1934, in honor of Dr. Edgar Collins Bain, this morphology named as “bainite”. However, this name took some time to pass on to literature, so different names can be observed in earlier researches such as unnamed, dark etching, acicular aggregate somewhat similar to martensite (1936), a rapid etching acicular structure (1939), austempered structures (1940). In **Figure 2-1**, microstructures of eutectoid steel are given.

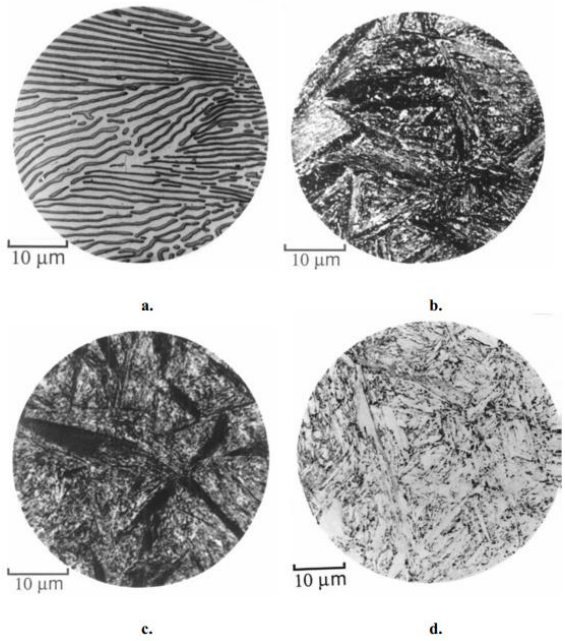

Figure 2-1 Microstructure visions of eutectoid steel a. Pearlite formation at 720oC b. Bainite obtained with isothermal transformation at 290oC c. Bainite obtained with isothermal transformation at 180oC d. Martensite [4]

2.1.1. Bainite Transformation

Bainite is composed of ferrite and cementite (Fe_3C). This tough and ductile microstructure forms when steel is isothermally treated below pearlite nose and above martensite start temperature. During cooling, austenite transform is controlled by diffusion and pearlite formation is not allowed. In addition, cooling rate does not allow diffusionless transformation, which causes martensite formation. [5]

In **Figure 2-2**, Time-Temperature-Transformation (TTT) diagram shows required conditions in order to form bainite. Above temperatures of pearlite nose between 530 and 727 ^{o}C austenite transforms pearlite. Below temperatures of pearlite nose between 220 and 530 ^{o}C, when steel is isothermally treated austenite transforms bainite.

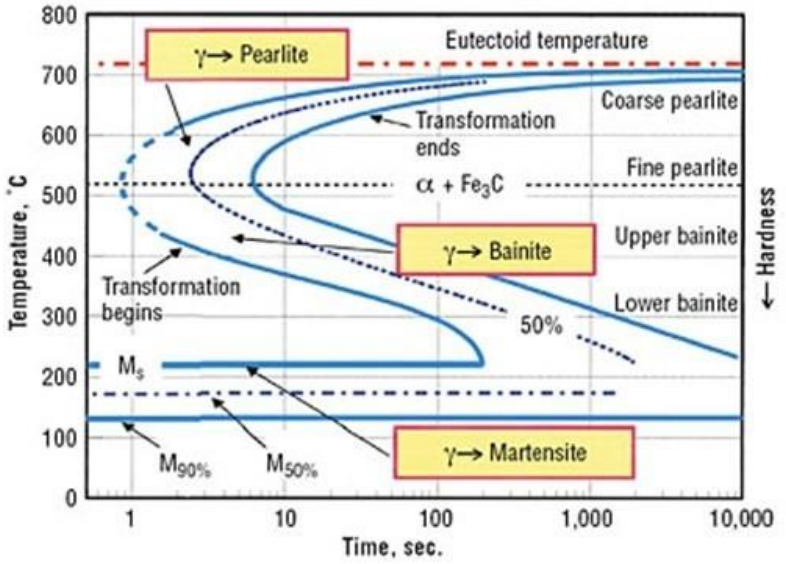

Figure 2-2 TTT diagram of eutectoid steel (γ: Austenite, Ms: Martensite start)[6]

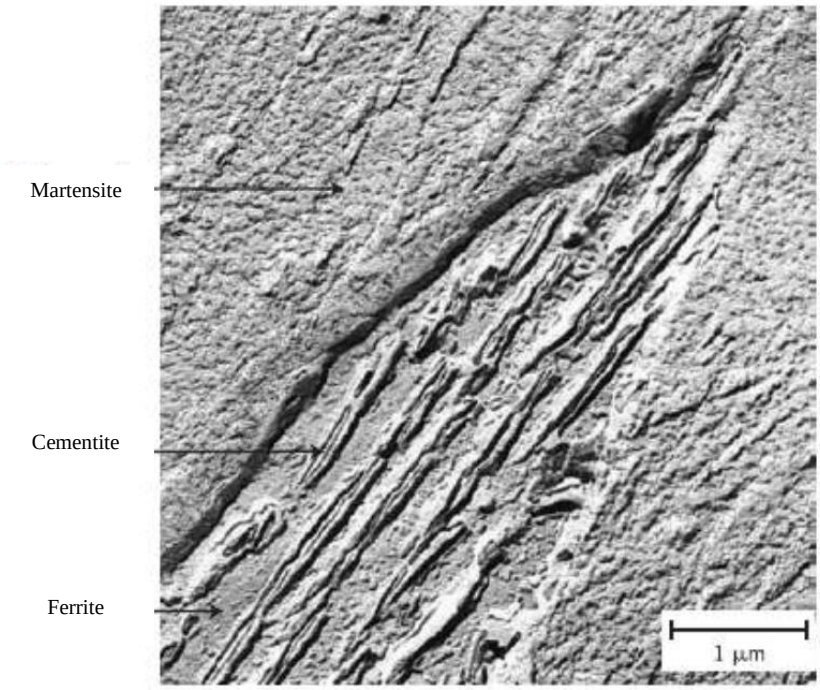

Figure 2-3 Bainite under Scanning Electron Microscope [7]

In **Figure 2-3**, bainite morphology can be seen under scanning electron microscope (SEM).

There are two different opinions about ferrite nucleation during transformation of austenite to bainite. One says that transformation mechanism is controlled by diffusion and by diffusion of carbon atoms ferrite nucleates and grows. Another one says, diffusionless slip occurs and ferrite nucleates like martensite formation. [7,8]

Diffusion controlled mechanism:

According to Hultgrens, bainite occurs as parallel plates of Widmanstatten ferrite. Spaces between plates filled with composed of ferrite and cementite. First, ferrite nucleates and enriches austenite by carbon atoms. Between interface of ferrite and austenite phase cementite precipitates from austenite enriched by carbon atoms. In **Figure 2-4** growth of bainite is shown. [9, 10]

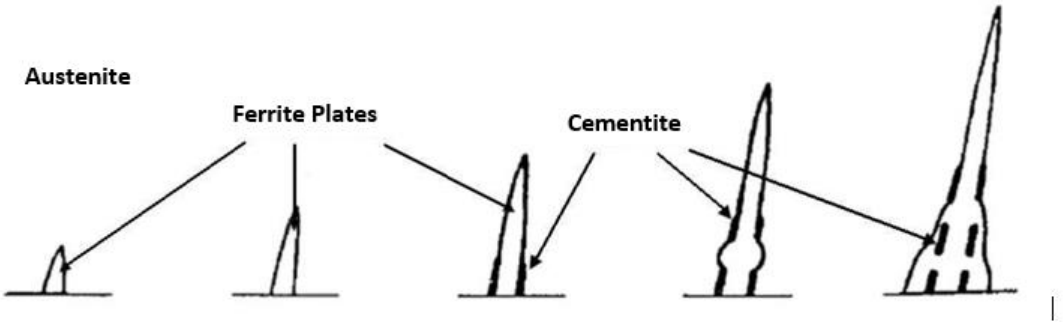

Figure 2-4 Lateral growth of bainite structure [9]

Growth velocity of ferrite plates are directly related with diffusion of carbon atoms. Carbon content of ferrite phase is determined by equilibrium of ferrite-austenite interface region. According to cementite precipitation carbon content decreases and lateral growth occurs. Therefore, growth of cementite and ferrite related with each other. Growth stops when plates are blocked by grain or twin boundaries. According to Hillert, diffusion controlled bainite formation process is supported by the below mentioned findings [9, 11]:

- Experimental transformation rates show Widmanstatten ferrite and bainite region occur similar mechanism
- There is no proof that bainitic ferrite is excessively saturated
- There is no experimental result that high transformation rates are needed during bainite formation
- There is no relationship between characteristic features of ferrite-austenite interface and plate martensite interface

2.1.2. Bainite morphology

Bainite is basically composed of ferrite and cementite and also may contain retained austenite and martensite. Different morphologies can be obtained by changing heat treatment conditions or chemical composition of steel. In order to classify phases in bainite appropriately SEM or TEM should be used. Because of the low resolution of optical microscope, bainite can be classified as follows [9]:

- Upper bainite
- Lower bainite
- Granular bainite

In bainite, according to composition of steel, there might be carbides, carbon-enriched retained austenite, martensite or martensite-retained austenite (M/A) microstructure [9].

Carbides are shown when Al or Si wt% is less than 1%. These carbides occur as cementite Fe_3C. However, it can be seen as $Fe_{2,4}C$ in lower bainite. Cementite form from carbon-enriched retained austenite or directly from austenite. In lower bainite, these cementites precipitate in or between bainitic ferrites. If the effect of isothermal transformation temperature is considered, lower the temperature smaller and more the carbides (Fe_3C) are obtained. Therefore, the effect of precipitation increases. Moreover, if transformation is obtained by continuous cooling, finer cementite

precipitates are obtained when they are compared with isothermally treated. Because, in continuous cooling transformation time range is much more lower. [4, 6, 12, 13]

Retained austenite or M/A microstructure are observed when carbide precipitates are suppressed with addition of aluminum or silicon. Carbon atoms remain in austenite and increase the carbon content of these regions. As a result, martensite start formation temperature decreases and austenite remains in microstructure at room temperature. If carbon-enrichment is not provided in steel with addition of aluminum or silicon, remaining austenite transforms into martensite since, austenite is not a stable phase at room temperature. In austenite different carbon content is seen during diffusion of carbon atoms, so both martensite and retained austenite are observed in microstructure which is called as martensite-austenite microstructure "M/A". Generally, there are two types of M/A transformation in bainite. One is obtained between bainite clusters, which is called bulky retained austenite, the other one is seen between bainitic ferrite plates as thin film. In **Figure 2-5**, both M/A morphology are shown. The formation and ratio of M/A phase contributes mechanical properties of steel. Higher toughness values are get when M/A phase is obtained between bainitic ferrite plates. Ratio and features of M/A phase differs on parameters such as transformation time, temperature, alloying elements and carbon content of steel [6, 9 and 14].

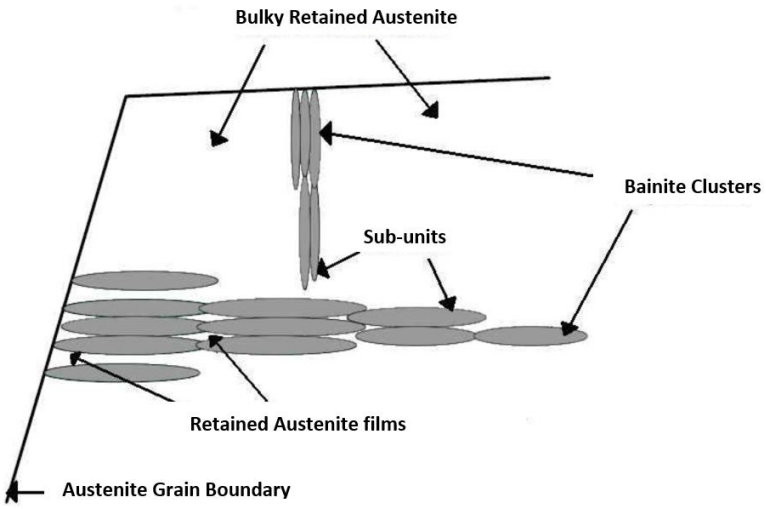

Figure 2-5 Bulky and thin film structure of retained austenite in bainite morphology [9]

2.1.3. Stability of retained austenite

Retained austenite is found as secondary phase in bainite and it cause hardening because of martensite transformation as TRIP steels. For example, under repeated stresses retained austenite inhibits propagation of fatigue cracks. Because of martensite transformation in retained austenite, volume expands and some residual stresses occur in steel, which retards or stops crack propagation. So the stability of retained austenite phase can be characterized as internal and externals factors. Internal factors can be listed as austenite grain size, morphology, chemical composition and crystallographic orientation. On the other hand, external factors are position of austenite grains, hardness of surroundings, stress and micro-stress distribution [9, 15-18].

Internal factors:

The most essential internal factor is chemical composition. Carbon content of austenite is higher than bainitic ferrite. As a result, martensite start formation

temperature decreases and austenite remains as metastable phase at room temperature. Wang and his colleagues found a relationship between weight percent of carbon and martensite start temperature. This relation is given as equation below. [9, 19, 20]

$M_s = 273 + 545,8.e^{-1,362 \cdot wc}$

Also, silicon and manganese have effects on retained austenite. When silicon is higher than 1% carbide formation is suppressed and stabilize retained austenite phase. In addition, manganese is added as austenite stabilizer in steel. [21]

The other internal factor in retained austenite is morphology of austenite which is also called mechanical stability. As it is mentioned before, retained austenite can be seen as bulky between bainite clusters or like thin film between bainitic ferrite plates. Austenite films are mostly isolated from bainitic ferrite. Carbon diffusion from austenite become difficult due to carbon solubility of ferrite phase. Retained austenite films between ferrite plates enriched by carbon and also chemical stabilization increases. Therefore, austenite films has higher chemical stabilization when it is compared with bulky retained austenite. Due to carbon content of retained austenite, its hardness becomes higher and stability increases. [9, 22, 23]

Austenitic grain size also effects stability of retained austenite as internal factor. Wang and his colleagues also show in their researches, if grain size is less than 0,01 μm stability of retained austenite increases. Lower grain sizes decreases martensite start temperature. Because due to interface energy between grains martensite formation retards in austenite grains. [9]

External factors:

The surrounding matrix of austenite grain is one of the important external factor that effects stability. Hardness of bainitic ferrite can be controlled by decreasing silicon addition and precipitation hardening. By precipitation, hardness increases in bainitic ferrite so volume expansion retards because of higher hardness values of ferrite. Xiong

and others observed when retained austenite films are surrounded by martensitic films, stability of retained austenite increases. In this case, martensitic films inhibit volume expansion due to its high strength values. [9]

Another external factor is stress distribution in surrounding matrix and microstructure. Small austenite grains cause small bainitic ferrite and internal stress level increases. As a result, stability of retained austenite increases and high elongation values can be get around 26%. .In case of ferrite has higher internal stress, during stress distribution of TRIP steel researches, Suh, Ryu and others show that austenite can only transforms martensite in high dislocation density. [9, 24, 25]

Position of austenite grains also effects stability of retained austenite. Stability of retained austenite near ferritic matrix interface differs from retained austenite in ferritic matrix. Retained austenite near ferritic matrix interface is highly stabilized and cannot be transformed even high deformation. [9]

2.1.4. Bainite classification

In 1930, Davenport and Bain investigated bainite under optical microscope and identified microstructure. Since, wide range of morphologies with wide range of mechanical properties it is hard to classify bainite clearly. In 1939, Mehl classified bainite as upper and lower bainite for isothermally treated steels. At high austempering temperatures upper bainite is obtained. Bainitic ferrite nucleates with very low content of carbon. During and after ferrite formation carbon diffuses into austenite and it forms carbides. These carbides precipitates between carbide plates and it takes place in carbon-enriched retained austenite phase. At low austempering temperatures lower bainite is obtained. Primary phase is again bainitic ferrite and carbides precipitates between ferrites and they also precipitates in ferrite with 55^{o}-60^{o} angle. The main difference between upper and lower bainite carbide precipitation is seen also in bainitic ferrites. In **Figure 2-6** the formation stages of upper and lower bainite can be

seen. In **Figure 2-7**, microstructure of lower and upper bainite are shown [4, 5, 9, 26 and 27].

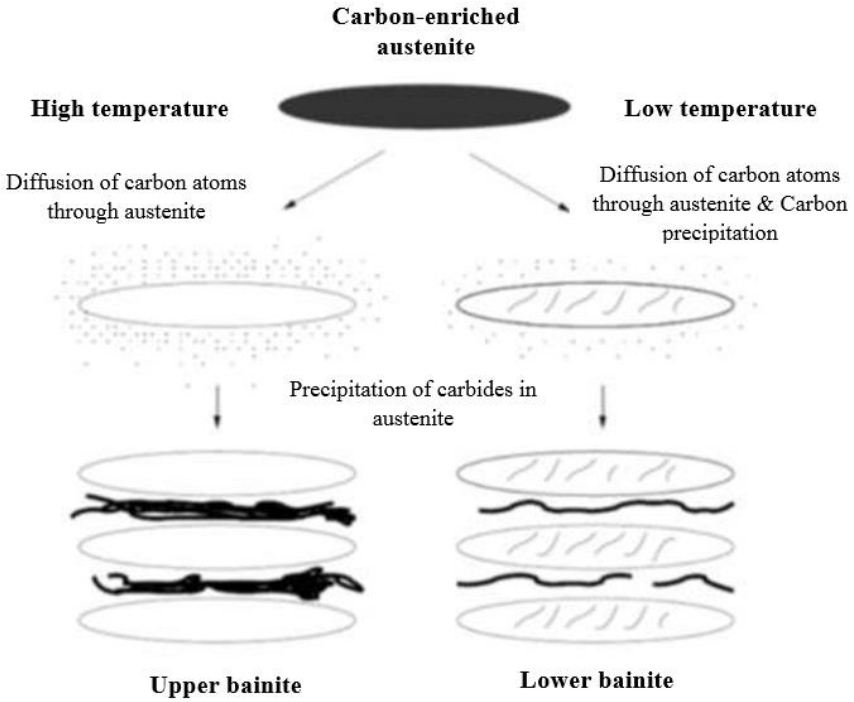

Figure 2-6 Transformation of upper and lower bainite schematically [4]

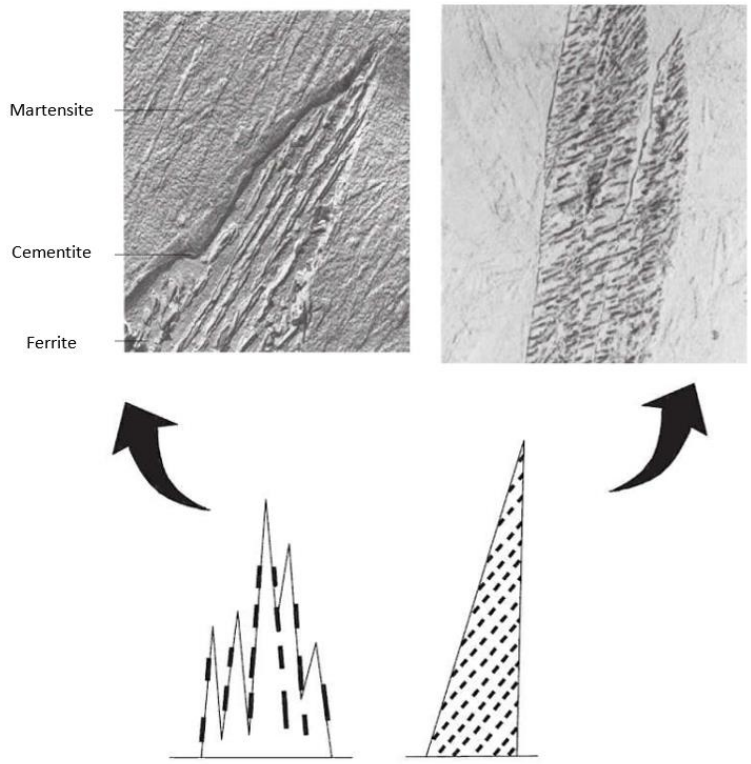

Figure 2-7 Microstructure of upper and lower bainite schematically [28]

Spanos and others claims, for Fe-C-%2Mn alloys different morphologies can be seen in bainite. They form at different temperatures and composition which is given in **Figure 2-8**. In addition to lower and upper bainite granular, longitudinal and transverse bainites can be observed in bainite morphology. Granular bainite generally seen in eutectoid and hypereutectoid steels' microstructure. Moreover, granular bainite is not limited with spherical shapes. They are related with internal morphology of bainite. Lack of carbides is the main characteristic of granular bainite. Carbon diffuses and enriches austenite from bainitic ferrite and granular bainite can contain any secondary phase that can transform from carbon-enriched austenite such as pearlite or cementite residue, bainite, M/A or martensite. Transverse bainite generally seen in eutectoid steels. [9]

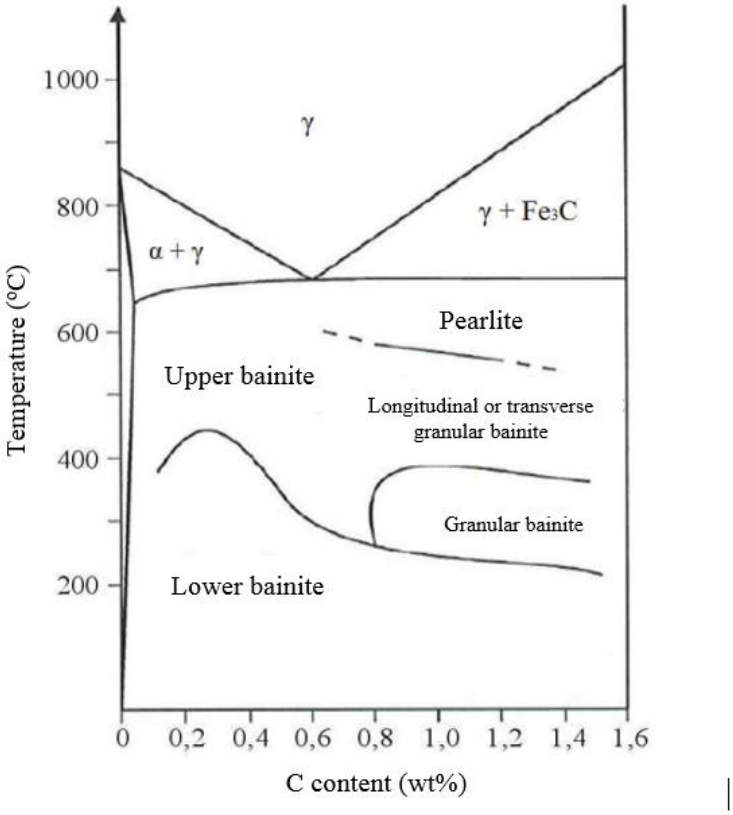

Figure 2-8 According to Spanos and others, bainite classes in different carbon content and temperature [9]

2.1.5. Mechanical Properties of Bainite

Wide range morphology of bainite provides different strength values and ductility properties. High-carbon-steel with lower bainite can exceed over 1400MPa and 55 HRc. These values mainly get from fine ferrite plates, high dislocation density and fine cementite distribution. The other factors that effect mechanical properties of bainite are alloying elements, precipitation hardening, carbide precipitation and thickness of bainitic ferrite. The effect of thickness of bainitic ferrite can be explained with Hall-Petch equation. Also thickness of bainitic ferrite directly related with dislocation and carbide density. [29]

$\sigma_y = \sigma_0 + K/\sqrt{d}$

According to Irvine and Pickering, there is a direct relation between decomposed carbon amount and hardness of bainitic steel. Hardness increases 190 HV for 1% of C in steel. Hardness of bainitic steels without carbides affected by austenitic phase or M/A phase. It increases depending on the carbon content and stability of retained austenite. By lowering transformation temperature, finer carbide precipitates occur and higher strength and hardness values are obtained. However, if carbides increase because of carbon content toughness of steel decreases. Retained austenite and bainitic ferrite has favorable effect on toughness. So it can be provided by silicon addition in steel to suppress carbide formation. Researchers also show that, upper bainitic steels have lower toughness and ductility when they are compared with lower bainitic steels. When austempered bainitic steels compared with quenched and tempered (Q&T) steels, they show higher toughness and elongation values. Martensite after quenching process is very hard and brittle. On **Table 2-1** some mechanical properties of AISI 1095 steel with different heat treatment processes can be seen [4, 9 and 29].

Table 2-1Mechanical properties of AISI 1095 steel at room temperature with different heat treatments

Heat Tretment	**Hardness (Rockwell C)**	**Toughness (J)**	**Elongation (%)**
Quench&Tempered	53,3	16,43	0
Quench&Tempered	52,4	19,17	0
Martempered	53,0	31,50	0
Martempered	52,8	32,87	0
Austempered	52,0	61,64	11
Austempered	52,5	54,79	8

2.1.6. The effect of alloying elements

Generally, the effect of alloying elements can be grouped as austenite stabilizer and ferrite stabilizer for iron-carbon compounds. Austenite stabilizers decrease the

temperature values of A_3 line and increase the area of austenite region. Ferrite stabilizers have vice versa effect. The alloying elements for iron-carbon compounds in terms of enthalpy change (ΔH) are given in **Figure 2-9** [9].

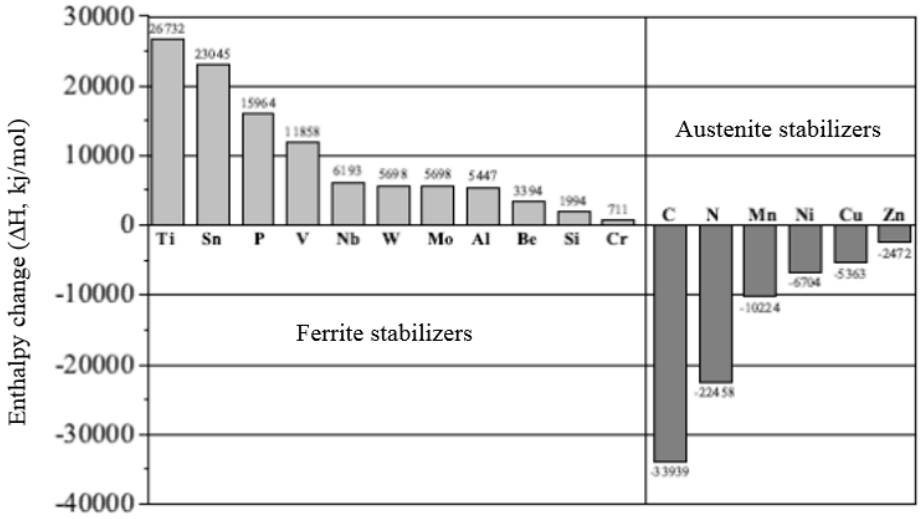

Figure 2-9 Austenite and ferrite stabilizer alloying elements and their effects in terms of ΔH [9]

2.1.6.1. Carbon

It is austenite stabilizer and has effects on transformation, microstructure and mechanical properties mainly. When carbon content in steel increases, bainite start temperature decreases and transformation time of bainite increases. Austenite has higher resolution of carbon than ferrite. Amount of carbide content also directly related with carbon amount in steel. Moreover, with higher carbon content, lower bainite can be obtained easier since the M_s temperature is lowered. If it is assumed that bainitic ferrite nucleates without diffusion, temperature value of T_0 is needed for transformation of bainite. Because, at this temperature, in same composition bainitic ferrite has lower enthalpy than austenite. In **Figure 2-10**, Bhadeshia shows T_0 term when bainitic ferrite and austenite have similar free energy. As it is seen in **Figure 2-**

10, T_0 curve is a function of carbon content. To occur ferrite-austenite transformation carbon contents is needed under T_0 curve. Above this curve, transformation is not possible thermodynamically. In summary, in order to provide growth of bainitic ferrite without diffusion, free energy of it should be kept just below the temperature T_0. This condition is proved by Caballero who measures carbon distribution in austenite with X-ray diffraction and atom probe tomography. [8, 9 and 30]

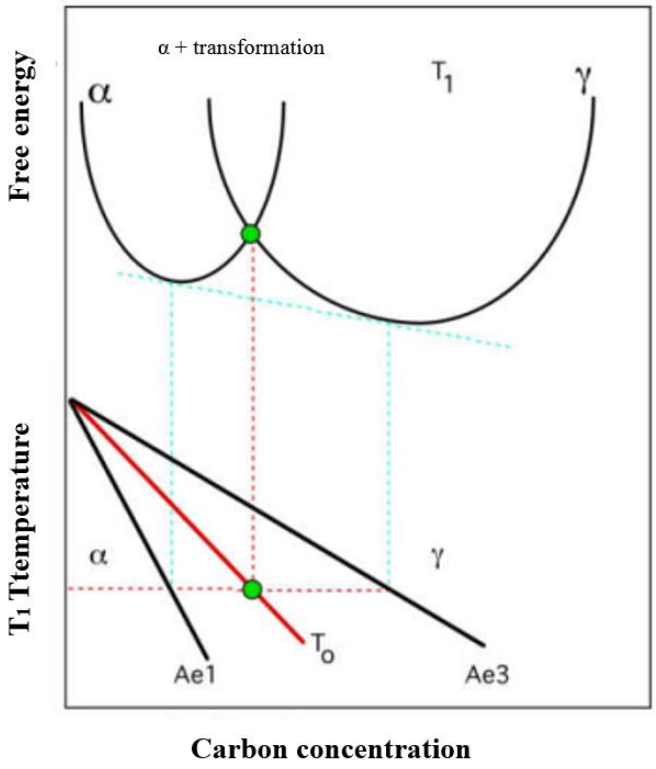

Figure 2-10 T_0 is shown in terms of carbon concentration and free energy for ferrite/austenite phase transformation [30]

2.1.6.2. Manganese

Manganese is used in steel generally over 0.5%. It is the third strongest austenite stabilizer element after carbon and nitrogen. It also shifts the TTT diagram to the right and down. As a result, bainite start, B_s, temperature is lowered and bainite transformation retards. The reason of that manganese has effect on austenite free energy. Gibbs free energy is lowered with increasing amount of manganese. In

addition, manganese has positive effect on hardenability in steel. However, there is risk of segregation during solidification from liquid steel. [9, 31]

2.1.6.3. Silicon

Silicon is one of the most crucial alloying element in bainitic steels. Over the amount of 1% silicon suppress carbide formation as it is seen in **Figure 2-11**. Cementite solubility is very low in the presence of silicon in steel. Separated carbon from bainitic ferrite enriches austenite and increase stability of retained austenite at room temperature. Moreover, silicon is a weak ferrite stabilizer and decreases free energy of ferrite. It has driving force for bainite transformation. [4, 9, 31-33]

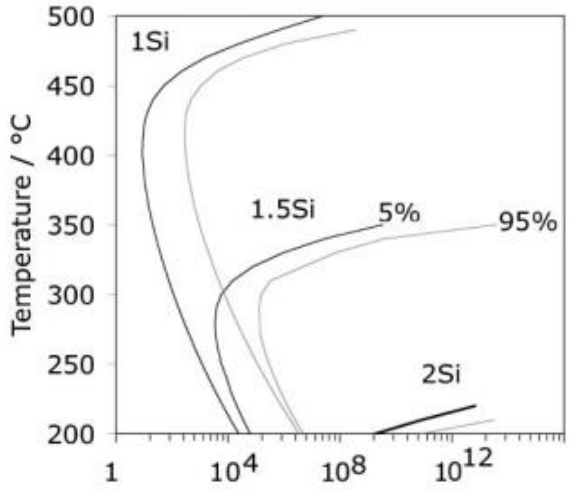

Figure 2-11 Cementite formation temperatures with different amount of Silicon content [34]

2.1.6.4. Chromium

Chromium is common used alloying element to contribute strength of steel. It is a weak ferrite stabilizer and strong carbide former. Chromium also decreases B_s temperature and retards formation of bainite but it retards ferrite formation more. It shifts TTT diagram to the right and it helps to obtain bainite with continuous cooling.

As a result, bainite formation takes longer time by decreasing Gibbs free energy. It also decreases martensite start temperature and critical cooling rate. [9, 35]

2.1.6.5. Molybdenum

Molybdenum is a ferrite stabilizer but it is used in steels in order to retard ferrite/pearlite formation. It forms carbides on austenite grain boundaries. So, nucleation for bainitic ferrite is blocked and full bainite transformation is not obtained. Moreover, bainite formation takes longer time. Over 0,5% molybdenum increases martensite start temperature. [9, 34]

2.1.6.6. Titanium, Aluminum, Niobium and Vanadium

Generally, titanium is used in boron steels. Because, titanium nitrides (TiN) or titanium carbonitrides (Ti (C, N)) bond with nitrogen atoms and boron does not precipitate as boron nitride in steel. Since, boron retards ferrite/pearlite formation, it increases hardenability of steel. Titanium is also used to obtain finer austenite grain size. Titanium nitrides block growth of austenite grains and smaller grains are occurred. However, TiN inclusions have sharp corners as it is seen in **Figure 2-12**. Excess amount of Ti has negative effects on mechanical properties especially on toughness. [8]

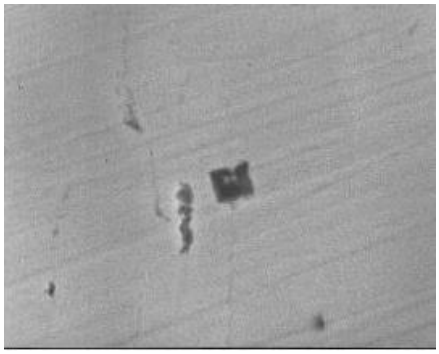

Figure 2-12 SEM image of TiN inclusion [34]

Aluminum is used as deoxidation and micro-alloying element in steelmaking process. It has high affinity with nitrogen and forms AlN compounds. So, austenite grain growth is inhibited and finer grains are obtained. Niobium has the highest effect on fine grain size. So, it increases mechanical properties. It is seen that 0,01% Nb addition in steel increases ultimate tensile strength about 35-40 Mpa. Vanadium has the highest solubility as micro-alloying element in steel. Depending on carbon content 0,01% V can improve UTS around 5-15Mpa. Solubility of vanadium can be controlled with nitrogen content. Vanadium has negative effect on toughness since, it has the lowest effect on fine grain size. In **Figure 2-13**, the effect on grain size of micro-alloying elements can be seen.

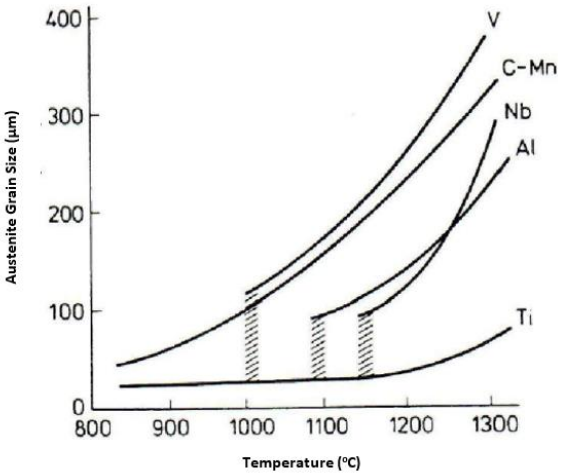

Figure 2-13 Effect of micro-alloying elements on austenitic grain size [38]

2.1.6.7. Boron

The effect of boron depends on if it is decomposed or precipitated. It retards ferrite and pearlite formation even if it is added in small amounts. Decomposed boron segregates through grain boundaries and nucleation retards. Thus, the activation energy needed for heterogeneous nucleation increases per unit area. Bainite is not influenced by this situation but it can be obtained by continuous cooling after boron

addition. However, if there is excess amount of boron, ferrite/pearlite transformation is not retarded. There are stable boron-oxides and boron-nitrides up to 1600ºC. These compounds should be eliminated from microscope by addition of Al and Ti. Al is added for deoxidation and Ti has higher affinity with nitrogen than boron. [4, 9, 39]

2.1.7. The effect of process

Austempering temperature and time have significant effect on stability of retained austenite and also mechanical properties of steel during bainite transformation. There are some researches how transformation temperature affects amount of retained austenite in bainite morphology. According to Hanzaki and others when isothermal transformation temperature is increased, amount and grain size of retained austenite increase. Thus, transformation temperature effects parameters that change stability of retained austenite. [9, 40]

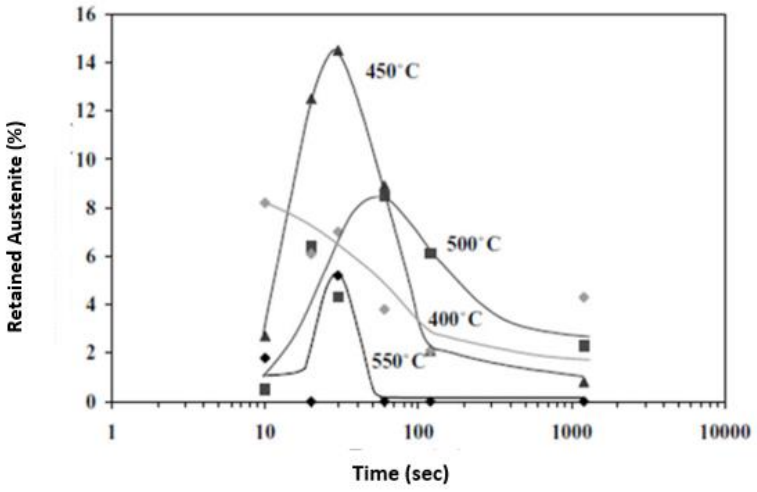

Figure 2-14 Retained austenite amount in terms of time and temperature [42]

Diaz-Fuentes and Gutierrez say that short transformation time about 10 to 40 seconds amount of retained austenite increases at high temperatures as it is seen in **Figure 2-14**. When transformation takes longer time bainitic ferrite amount increases. So, carbon content in austenite increases and transformation becomes stable Regions far

from bainitic ferrite transform martensite when they are quenched. When transformation time is kept about 40 to 1000 seconds retained austenite content decreases. Stability of retained austenite is lowered by increasing martensite start temperatures in local regions. Also, carbon precipitate for longer transformation time and retained austenite may become bainitic ferrite. [9, 41, 42]

In **Table 2.2**, Zhang and his colleagues are investigated mechanical properties of steel after isothermal bainitic transformation at 300ºC with different duration. Samples are kept different duration times at this temperature such as 30, 60, 90 and 120 minutes. As it is seen in **Table 2.2**, when transformation time is increased strength decreases but elongation increases because of amount of retained austenite. [9, 43]

Table 2-2 Effects of bainite transformation time on tensile strength, elongation and amount of retained austenite [43]

Bainite Transformation Time (min)	**Tensile Strength (MPa)**	**Elongation (%)**	**Amount of Retained Austenite (%)**
30	1727	2,6	5,4
60	1731	7,7	18,6
90	1668	8,4	18,7
120	1535	11,4	31,3

2.1.8. The Effect of Austenitic Grain Size on Bainite Transformation

Since, bainitic steels have high tensile strength and toughness with their ductile behavior; they are used in too many different areas that these properties are required. Strength is mainly provided from bainitic ferrite, ductility is controlled by retained austenite in steel. Austenitizing temperature is one of the essential parameter that is directly affect austenite grain size. Bainite clusters starts forming from grain boundaries, so it determines the bainite morphology as it is seen in **Figure 2-15**. As a result, first austenite grain size must be controlled with austenitizing temperature. [4]

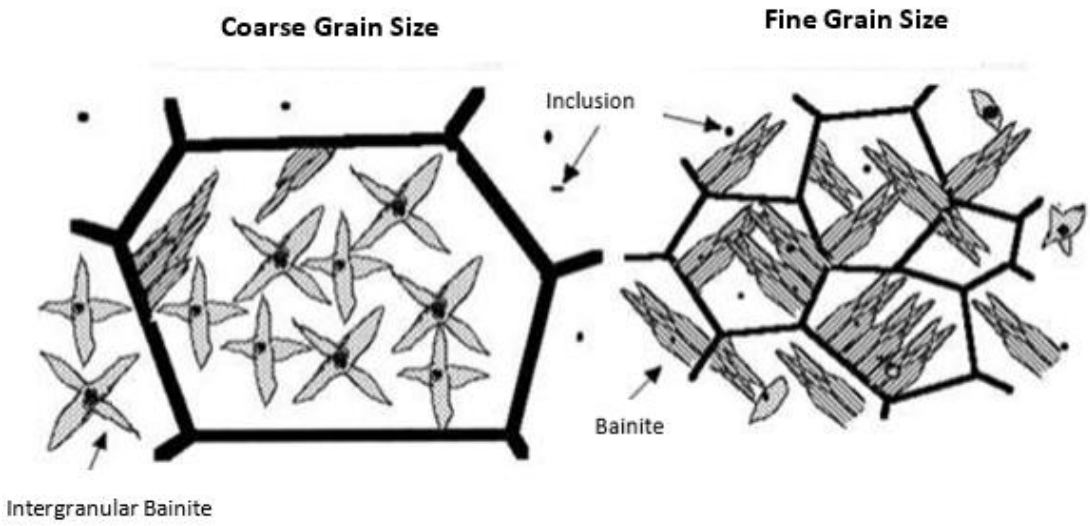

Figure 2-15 Effect of austenite grain size on bainite morphology [4]

According to Beata, mechanical properties such as strength and toughness decrease when austenitizing temperature is higher and they are shown in **Figure 2-16** and **Table 2-3**. [44]

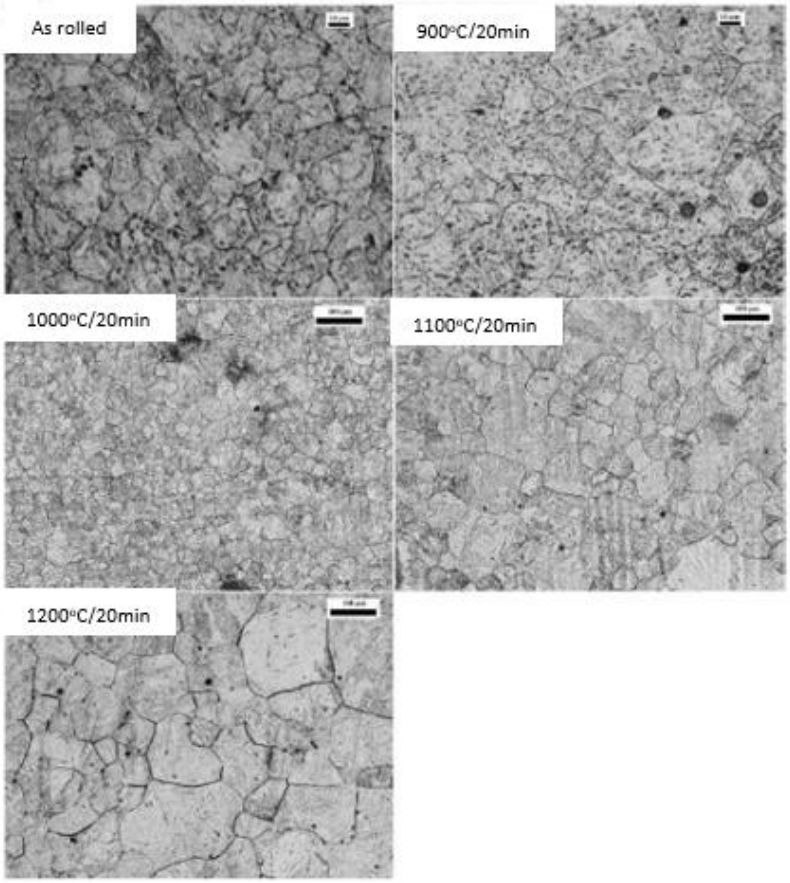

Figure 2-16 Microstructure images of samples austenitized for 20 minutes at different temperatures [44]

Table 2-3 Effects of austenitizing temperature [44]

Austentizing Temperature (ºC)	**Tensile Strength (MPa)**	**Yield Strength (MPa)**	**Elongation (%)**	**Toughness (J/cm^2)**
As rolled	1433	1106	14,6	70
900	1445	1076	14,1	49
1000	1413	1016	13,2	38
1100	1425	1006	12,9	30
1200	1382	987	12,6	19

2.1.9. Bainitic Forging Steels

In recent years, latest developments are mostly consider fuel consumption and gas emissions. For light vehicles, different kind of materials are experimented on vehicles. Quenched and tempered steels have better mechanical properties than pearlitic-ferritic steels. However, production rate of Q&T steels are slower and they are more expensive than pearlitic-ferritic steels. High strength and ductile bainitic steels can bridge the gap between Q&T steels and age hardened ferritic pearlitic (AFP) steels. [45-47]

2.1.9.1. Chemical Compositions of Bainitic Forging Steels

High performance automotive parts generally made from quenched and tempered steels or from precipitation hardened ferritic-pearlitic steels in order to give strength and improve fatigue life. In ferritic-pearlitic steels, micro alloying elements such as Nb, Ti or V can be added to improve mechanical properties. [46, 48]

Bainitic steels are used for high strength applications while sustaining adequate toughness. In microstructure of forged bainitic steels, primary phase is bainitic ferrite sheaves. If there is 1,5%Si or more, no carbide precipitation is seen within the bainite sheaves. The retardation of carbide precipitation results in rejection of carbon atoms into the austenite and causes oversaturation of austenite. As a result, retained austenite films are generally seen between the sheaves which contributes the toughness of the carbide free bainitic steels. In order to increase strength of bainitic steels:

- Volume fraction of ferrite must be suppressed during cooling.
- Distance between bainite sheaves (λ) must be finer.
- In addition to vanadium, micro alloying elements Nb and Ti can be added for refining the grain size.

Mn is generally present for stabilizing the austenite phase.

In **Table 2-4** chemical composition of some forging bainitic steels are given such as 20MnCrMo7, 18MNCr5-3, 25MnCrSiVB6, 16MnCr5, HSX 130HD, HDB, 20MnCr5. [45]

Table 2-4 Chemical compositions of different bainitic forging steel grades [45]

Steel	**C%**	**Si%**	**Mn%**	**Cr%**
20MnCrMo7	0,22	0,50	1,72	1,60
18MNCr5-3	<0,20	-	<1,90	<1,50
25MnCrSiVB6	0,25	0,90	1,30	0,80
16MnCr5	0,16	-	1,25	1,00
HSX 130HD	0,17	1,20	1,50	1,20
HDB	0,17	1,50	1,50	1,30
20MnCr5	0,20	0,50	1,30	1,10

In addition to chemical composition, dimensions of part and appropriate cooling conditions is very important parameters. To obtain homogeneous and fine microstructure cooling system must be arranged carefully. [44]

2.1.9.2. Production of Bainitic Forging Steels

Safety parts and cyclic-loaded parts are required to have high strength and toughness. Quenched and tempered 42CrMo4 is generally used in automotive industry, since it comprehends these requirements. In order to lower the cost of production, the quenching and tempering step is tried to be omitted. In 1980s, vanadium is added to ferritic pearlitic forging steels for precipitation strengthening. Thus, precipitation hardened steels are obtained. 38MnVS6 contains 0,1%V in steel and it is used as an alternative steel to quenched tempered steels. [45]

Full bainitic microstructure can be obtained by isothermally treating just above the martensite start temperature of the steel, which is called “austempering”. After austempering, steel is quenched at room temperature. Full bainitic microstructure can be obtained with continuous cooling in forging quality bainitic steels, which brings an important advantage as far as the cost is concerned, as it is seen in **Figure 2-17**. However, it is hard to get homogeneous microstructure due to continuous cooling. If

it cannot be controlled during production, required mechanical properties may not be obtained. Martensite or upper bainite mixtures can be seen in microstructure. [49]

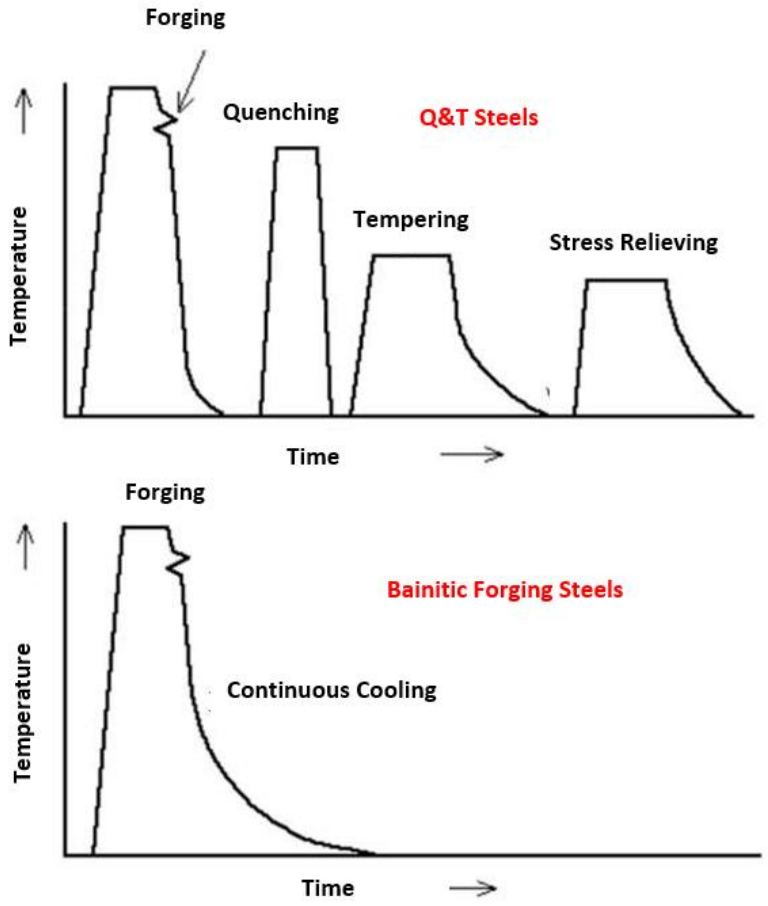

Figure 2-17 Applied heat treatments for Q&T steels and bainitic steels after forging

CHAPTER 3

EXPERIMENTAL PROCEDURE

3.1. Chemical Composition

There is a commercial steel used as a bainitic steel in applications requiring both high strength and toughness. This steel is named as REFERENCE STEEL. In the light of literature search and reference steel grade, experiment was started with deciding the composition of new steel grade. One base composition was determined with 5 alternative compositions and 1 reference steel grade is tested. Base composition is named as G1 and the alternative compositions are G2, G3, G4, G5 and G6. The compositions are given **Table 3-1**.

Table 3-1 Determined chemical composition of new alloys

CAST GRADE	C%	Si%	Mn%	P%	S%	Cr%+ Mo%	Ni%	V%	Al%	B%	Ti%	Nb%	Ca%	N%	Co%	Cu%
G1	0,22	1,40	1,50	0,010	0,070	1,45	0,05	0,00	0,010	0,0030	0,0200	0,0350	0,0005	0,0060	0,0100	0,06
G2	0,22	1,40	1,50	0,010	0,090	1,45	0,05	0,00	0,010	0,0030	0,0200	0,0350	0,0005	0,0060	0,0100	0,06
G3	0,22	1,40	1,50	0,010	0,050	1,45	0,05	0,00	0,010	0,0030	0,0200	0,0350	0,0005	0,0060	0,0100	0,06
G4	0,22	1,40	1,50	0,010	0,070	1,45	0,05	0,00	0,010	0,0030	0,0100	0,0350	0,0005	0,0060	0,0100	0,06
G5	0,22	1,40	1,50	0,010	0,070	1,45	0,05	0,00	0,010	0,0030	0,0200	0,0500	0,0005	0,0060	0,0100	0,06
G6	0,22	1,40	1,50	0,010	0,070	1,45	0,05	0,00	0,010	0,0030	0,0100	0,0500	0,0005	0,0060	0,0100	0,06
Ref. Steel Grade	0,28	1,11	1,49	0,008	0,060	1,02	0,19	0,05	0,022	0,0032	0,0280	0,0046	0,0003	0,0039	0,0130	0,17

G1, G4, G5 and G6 are designed with different amount of titanium and niobium additions. They are used as micro-alloying elements and it is known that they have a strong effect in grain refinement, which effects mechanical properties of experimental steel grades.

G2 and G3 differ from G1 with their sulphur content and only used for machinability test. In this study, they were not investigated in terms of mechanical properties and metallographic examination.

In **Table 3-2,** number of casts are shown for each steel grade. 20MnCr5, which has the closest chemical composition to new steel grades, is used before addition of alloying elements during casting. Total samples were taken from ingot casts of G1, G4, G5, G6 and reference steel grade are as follows:

- 3 tensile test samples
- 1 charpy impact test sample
- 5 machinability test samples
- Metallography and XRD samples
- Dilatometer samples

Table 3-2 Number of cast for each grades

Steel Grades	Differences	Total casts
G1	New main alloy	**5**
G4	Ti content decreased	**5**
G5	Nb content increased	**5**
G6	Ti content decreased Nb content increased	**5**
Ref. Steel Grade	Steel in use	**3**
Total		**23**

3.1.1. CCT diagrams

After research of alloying elements and their effects on mechanical properties and bainite morphology, CCT diagrams are drawn on a computer based program Jmatpro version 10.1. Also, composition of reference steel grade is integrated for comparison.

3.2. Production

All the steels were melted in induction furnace. They were vacuum treated in ÇEMTAŞ A.Ş. and casted (**Figure 3-1** and **Figure 3-2**). Al_2O_3 is used as refractory in furnace.

Figure 3-1 Induction furnace

Figure 3-2 Vacuum tank

After melting, 80x80mm section with 110mm height mould was used for solidification process as it is seen in **Figure 3-3**. In **Figure 3-4**, mould heater is seen which heats up mould to around 350^{o}C in order to prevent solidification problems and increase mould life-time. Temperature control was made by connected thermocouples to the heater.

Figure 3-3 80x80x110mm mould

Figure 3-4 Mould heater

Chemical composition of steels was checked with spectrometer ARL 4460.

3.3. Sample Preparation

After ingot casting samples were prepared for sampling as it is seen in **Figure 3-5**. Each steel grade was forged from 80x80x110mm to 40x40x400 around 1200ºC. Since the first geometry is not symmetrical, samples were machined and divided into two. Divided samples were forged from 40x40x200mm to 25x25x250mm around 1200ºC. Deformation is 61% and reduction ratio is around 2.5:1.

Samples of six new steel grades and reference steel grade were tested in terms of mechanical properties, microstructure, X-ray diffraction and CCT diagrams.

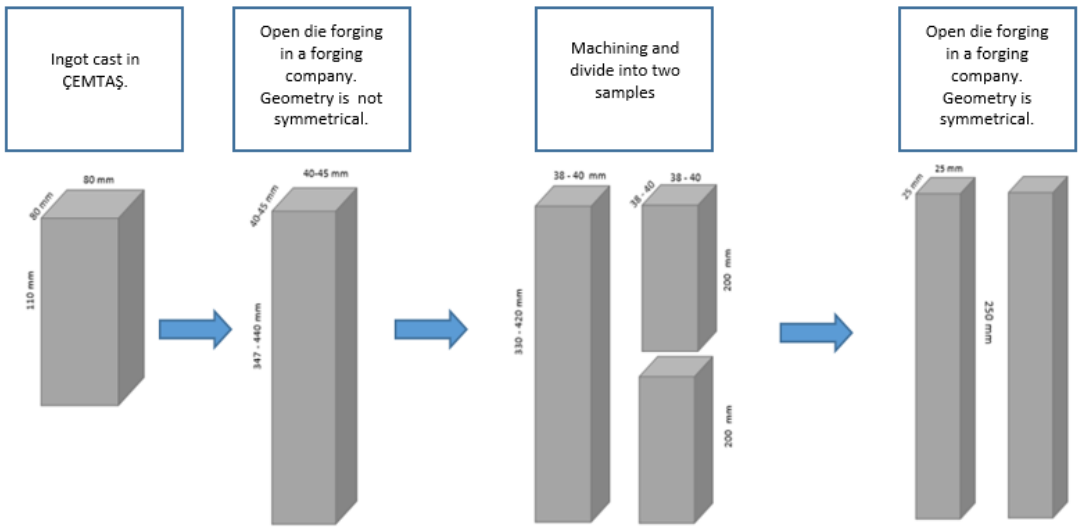

Figure 3-5 Sample shaping with forging and machining processes

3.3.1. Samples for mechanical tests

3 tensile test and 1 charpy impact test sample were taken from each steel grades except G2 and G3. Tensile test samples were prepared according to DIN EN ISO 6892-1 and charpy impact test samples according to DIN EN ISO 148-1. Tensile test was done with Zwick Z400 and charpy impact test was applied with Roell Amsler RKP 450. Also, hardness values were taken according to EN ISO 6506-1 and measured in terms of HB with EMCO TEST M5C-030.

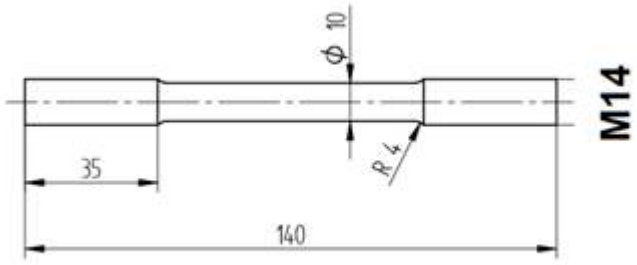

Figure 3-6 Tensile test sample dimensions

3.3.2. Metallography samples

Metallographic samples were taken from each cast for optical microscope and scanning electron microscope. Bainite, bainitic ferrite, retained austenite and also nitrides, carbides and their morphologies were investigated during study. Conventional metallographic methods were used in preparation of samples. Bainite thickness and austenite grain size of all grades were compared. Austenite grain size was measured according to ASTM E-112. The austenite grain size results were computed on a computer-based program called Clemex Vision PE.

3.3.3. Dilatometer samples

BAEHR Deformation dilatometer was used to obtain precise CCT diagrams of new steel grades and reference steel. Samples are heated up to 1200^{o}C and dimensional change is calculated upon cooling by dilatometer. Argon was used to arrange temperature decrease during test. It is significant to see bainite formation range with continuous cooling and it is compared with Jmatpro data. In **Figure 3-7**, requirements of dilatometer samples can be seen.

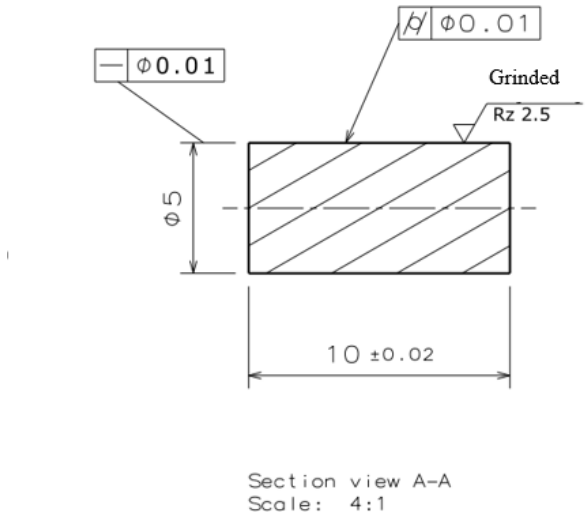

Figure 3-7 Dilatometer sample

3.3.4. X-ray diffraction samples

X-ray diffraction test was done to determine percentages of bainite and retained austenite in samples. Samples with 5mm-height were prepared in order to have accurate placement for the test. The results were computed on a computer-based program called X'Pert High Score Plus by using Cu-K α radiation.

CHAPTER 4

EXPERIMENTAL RESULTS

4.1. Alloy composition design

Alloying element contents were decided by considering the literature search. Composition of reference steel grade and new alloys are compared using Jmatpro CCT diagrams and shown in **Figure 4-1**. The compositions of the experimental alloys are given **Table 3-1**.

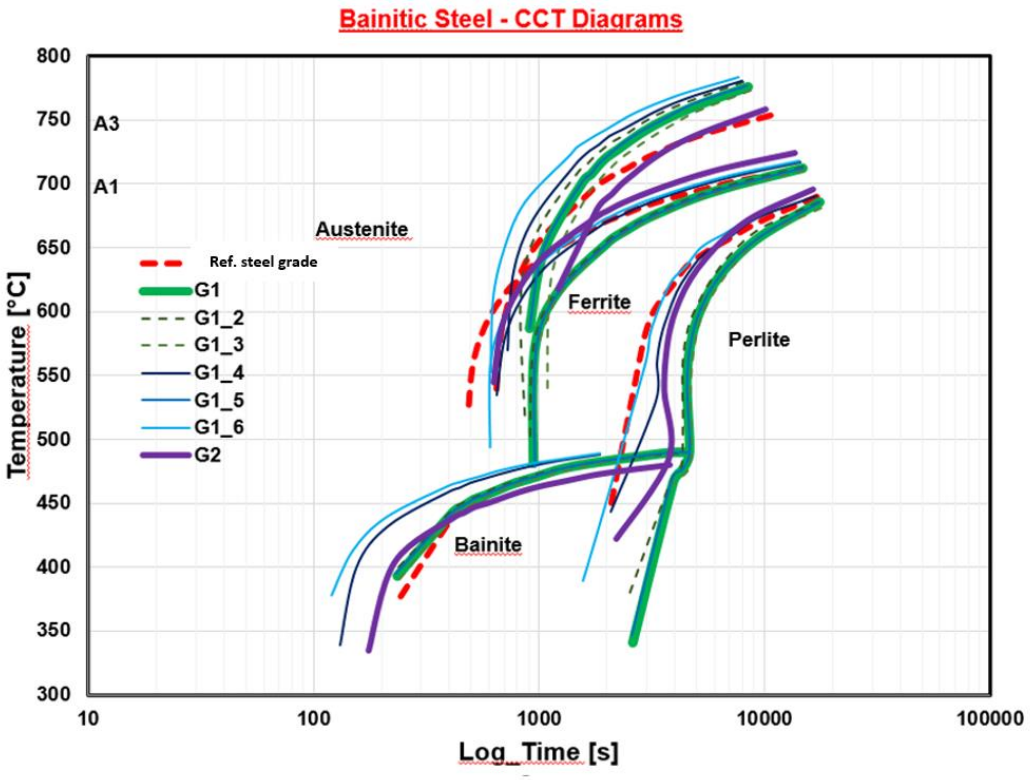

Figure 4-1 CCT diagram output from JmatPro

As it is seen from **Figure 4-1**, a larger bainite nose is obtained from alloy G1. Also with same cooling rate without changing process parameters, bainite microstructure can be obtained with new alloy design.

4.2. Metallographic Examinations

Microstructures of each cast was examined and they were compared with reference steel grade under both optical and scanning electron microscope after a continuous cooling heat treatment at a rate around 2-3K/sec which is the cooling rate of reference steel grade in process. Each steel grade is forged at 1200^{o}C.

Samples were used for austenite grain size measurement after microstructure examinations. Each steel grade is heated up to 1200^{o}C for 1 hour. They are carburized until 800^{o}C and quenched after 15 minutes at this temperature.

4.2.1. Optical microscope images

Steel grades were examined under 100x and 500x magnification. They were etched with 2% nital solution. The overall picture can be seen from figures between **Figure 4-2** and **Figure 4-5**. There is no inhomogeneity in the microstructure. In **Figure 4-6** to **Figure 4-9**, the micrographs show acicular bainite and martensite. There is no proeutectoid ferrite or pearlite in the microstructure. In order to decide if structure is bainite or martensite, SEM study is needed.

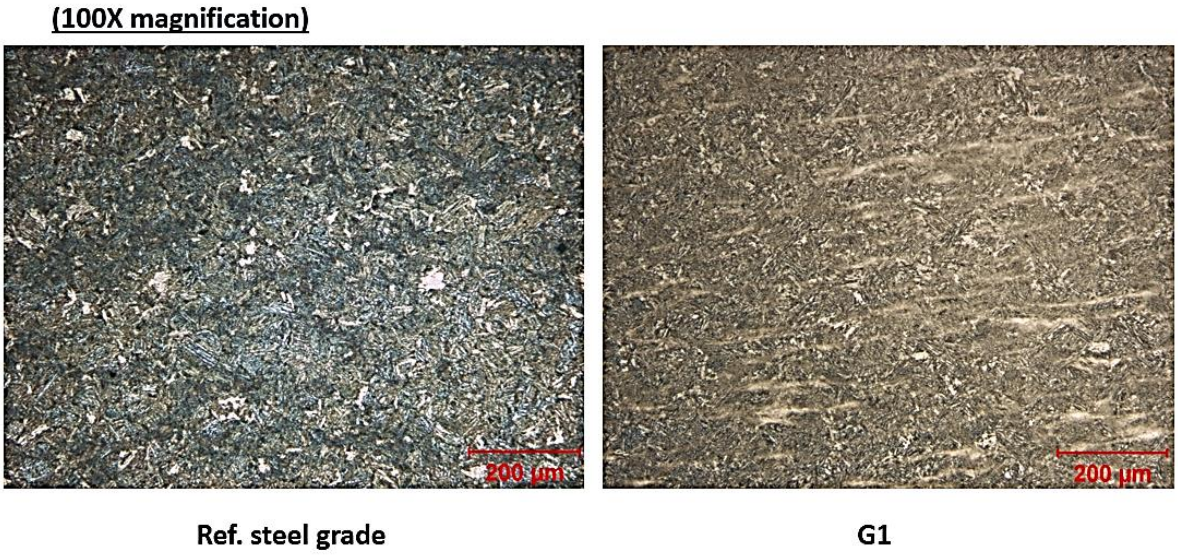

Figure 4-2 G1 vs Reference steel grade under optical microscope

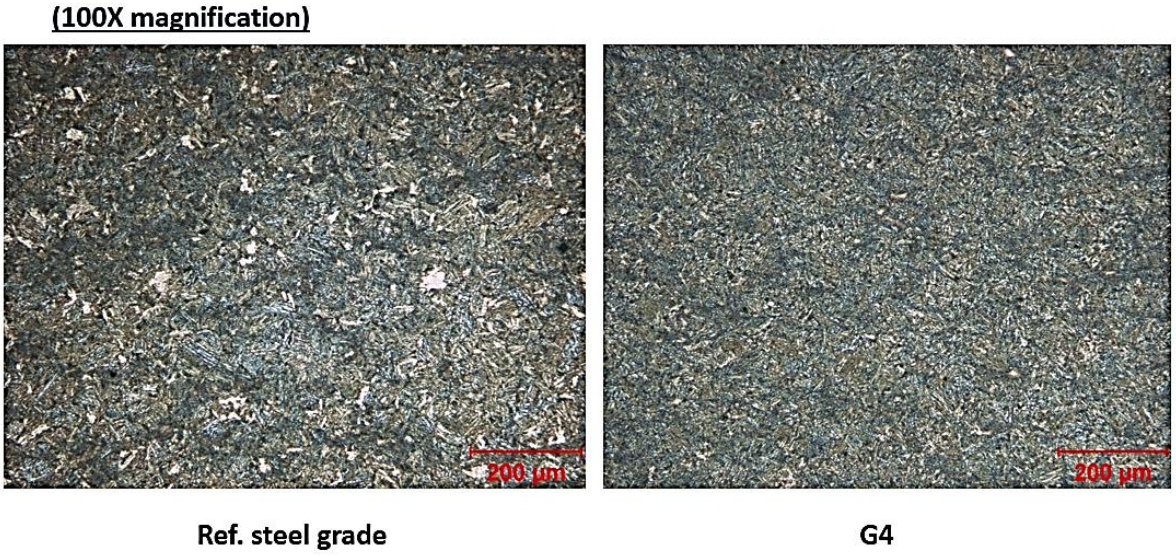

Figure 4-3 G4 vs Reference steel grade under optical microscope

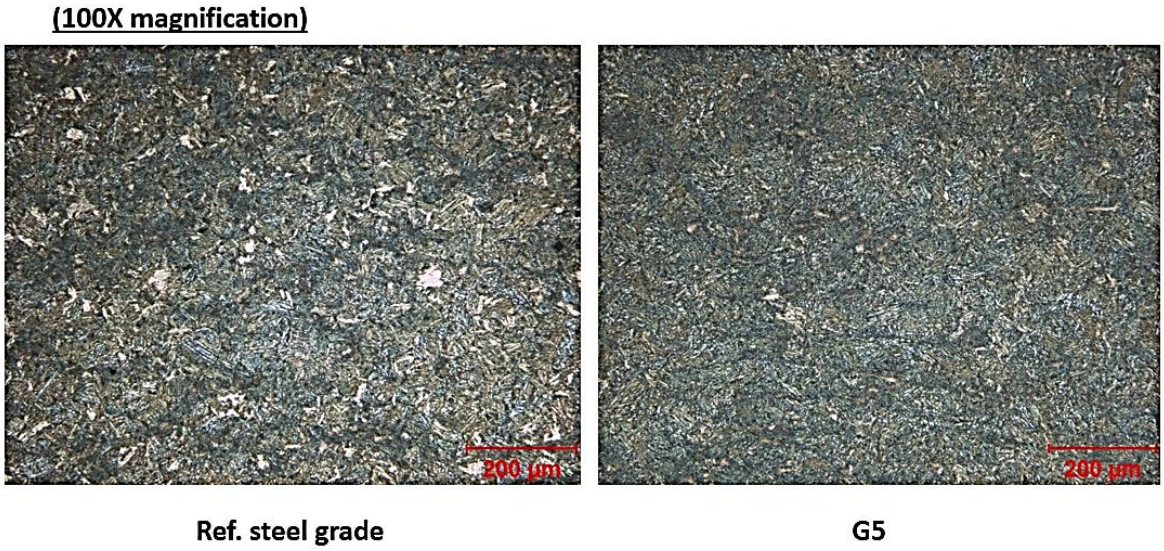

Figure 4-4 G5 vs Reference steel grade under optical microscope

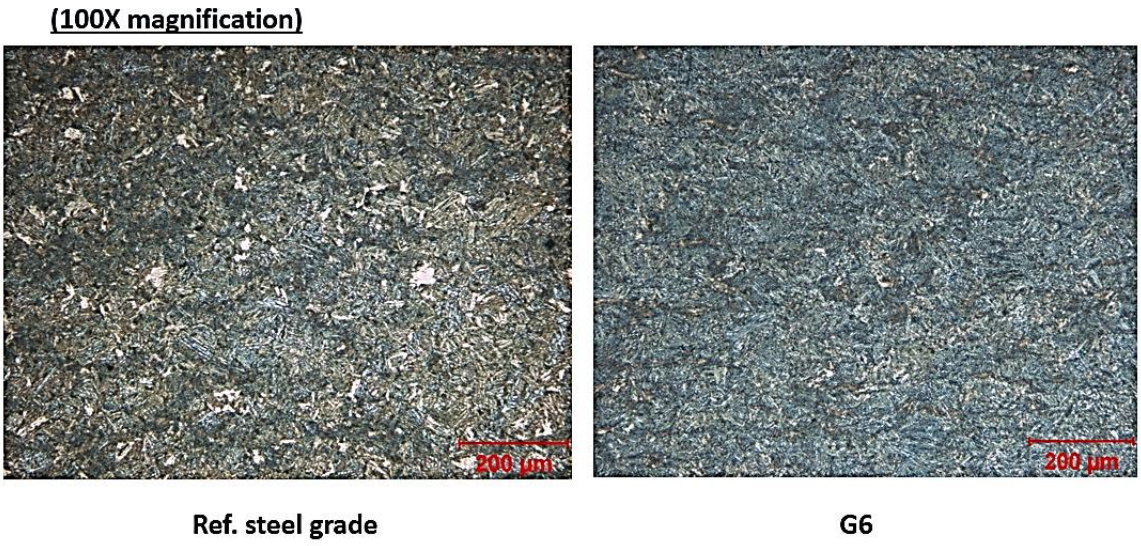

Figure 4-5 G6 vs Reference steel grade under optical microscope

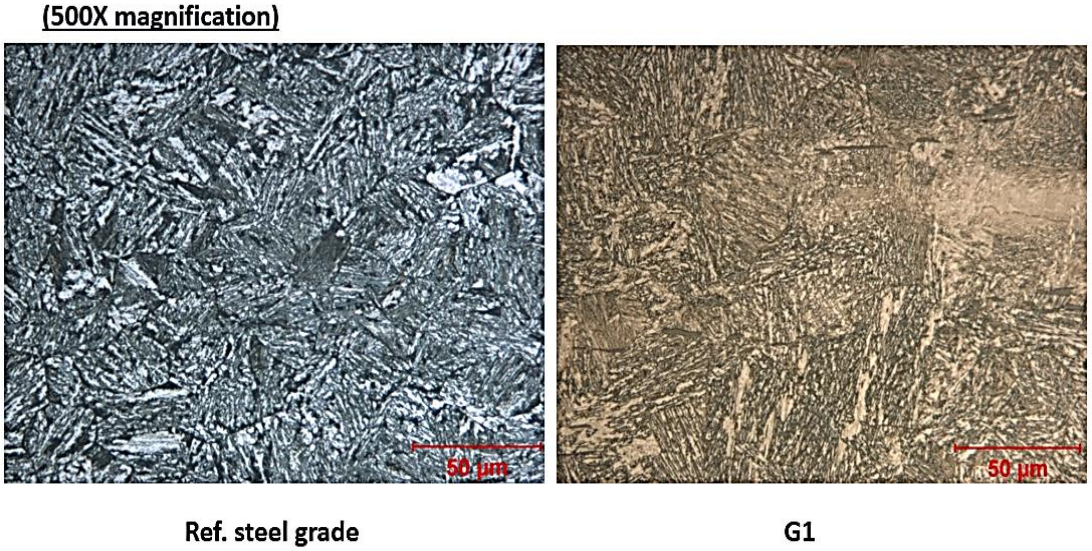

Figure 4-6 G1 vs Reference steel grade under optical microscope

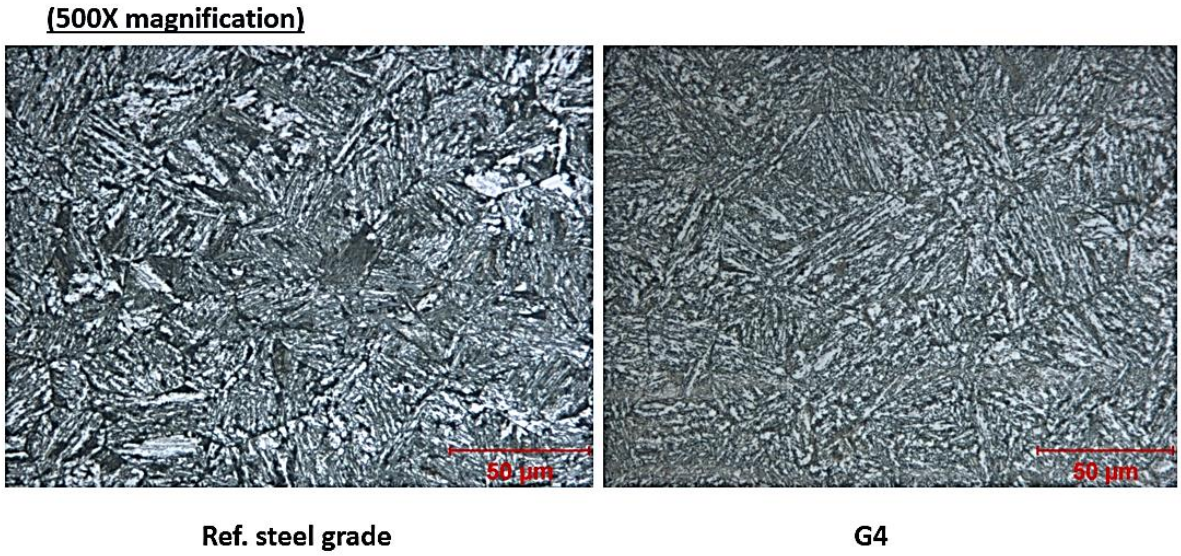

Figure 4-7 G4 vs Reference steel grade under optical microscope

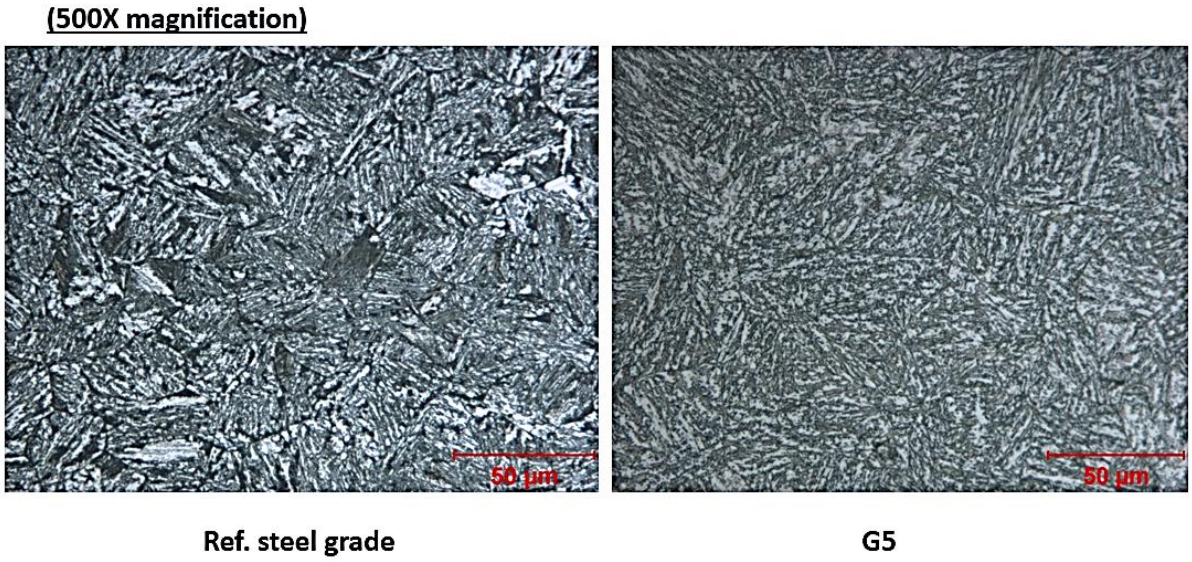

Figure 4-8 G5 vs Reference steel grade under optical microscope

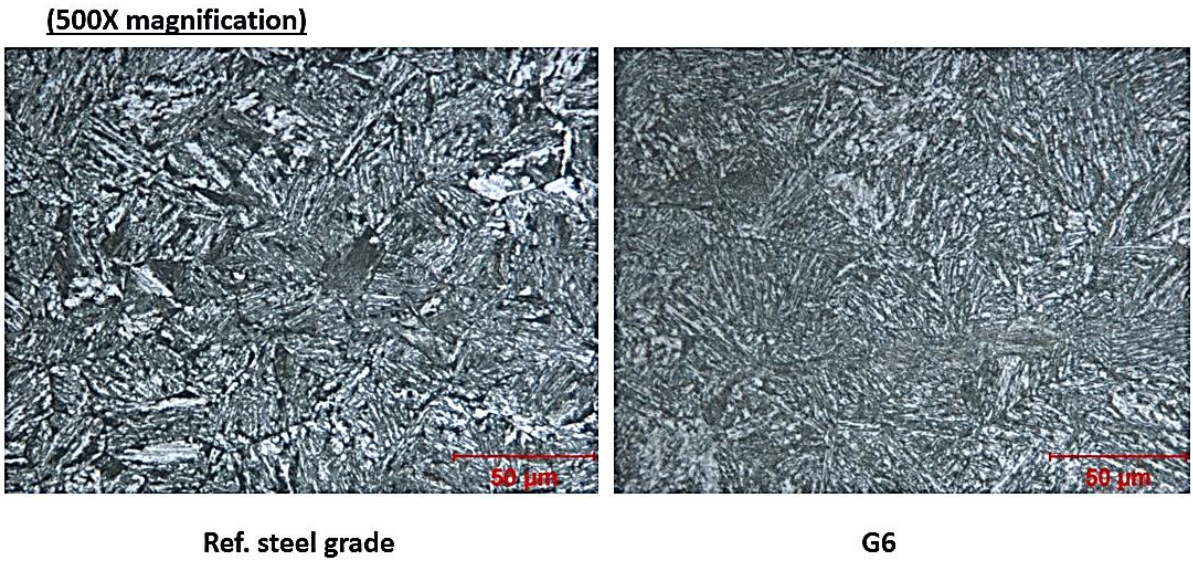

Figure 4-9 G6 vs Reference steel grade under optical microscope

4.2.2. SEM images

In order to make a detailed comparison between new grades and reference steel grade the specimens were observed under SEM. Present phases, bainite thickness and austenite grain size of each grade were compared. Each steel grade was forged around 1200^{o}C. Dimensional change after forging is given **Figure 3-5**. Percent reduction of area is 61%.

In **Figure 4-10**, reference steel grade is investigated. At higher magnifications blocky and flat type austenite islands between bainite sheaves are clearly seen, which are shown as M/A. As the austenite islands can retain as austenite or may transform to martensite, it is named as M/A. Reference steel grade has less silicon content than G series (1.10%). However, no carbides are encountered in microstructure of reference steel grade. Only bainitic ferrite phase can be seen.

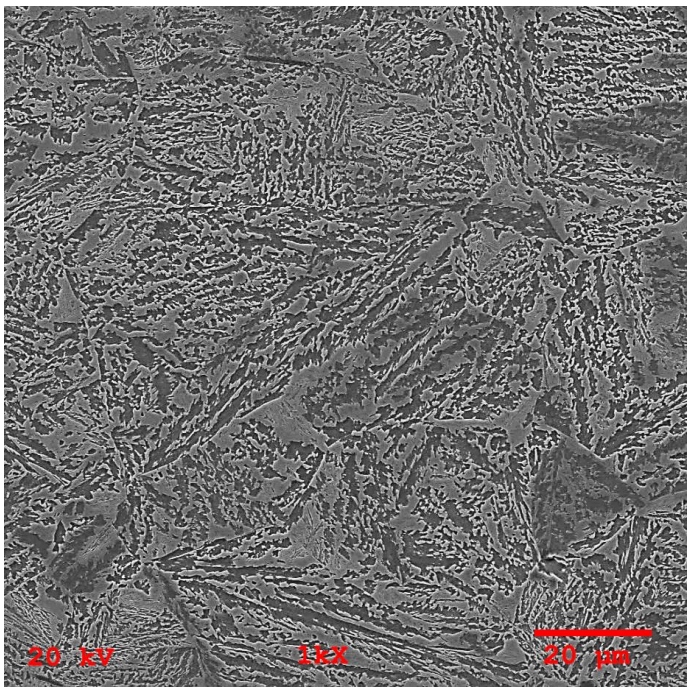

a.

*Figure 4-10 SEM micrographs of reference steel grade after hot forging and continuous cooling **a.** 1000x magnification **b.** 3000x magnification **c.** 5000x magnification*

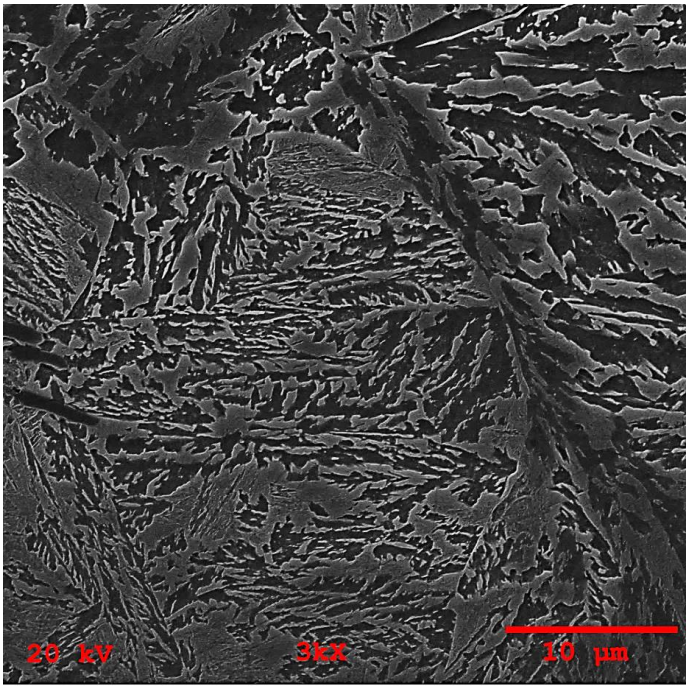

b.

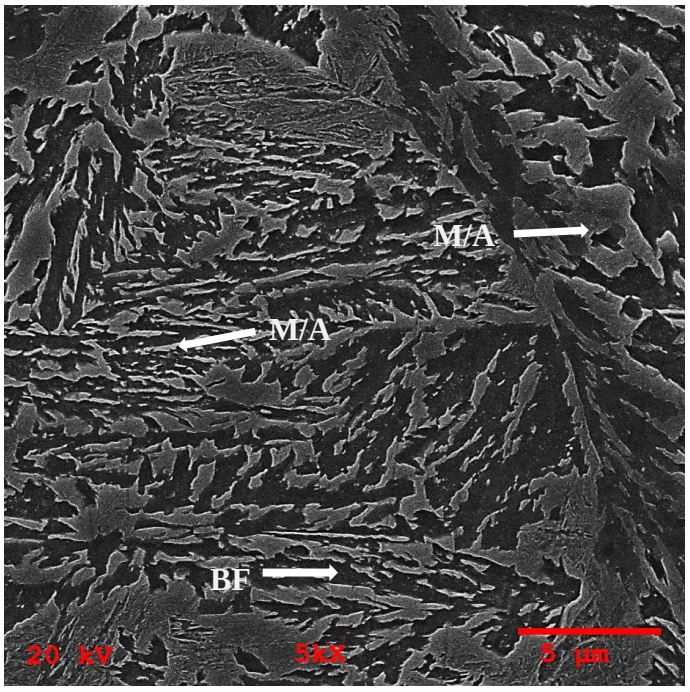

c.

Figure 4-10 (continued)

In **Figure 4-11,** the SEM micrographs of G1 steel grade is seen. At higher magnification, blocky retained austenite phases can be seen. The flat regions between the bainitic ferrite can be retained austenite films. Blocky M/A phases are seen as islands and they may transform to martensite upon cooling to room temperature. Carbides are not encountered in microstructure because of the high silicon content of steel (1.40%), so only bainitic ferrite phase is present.

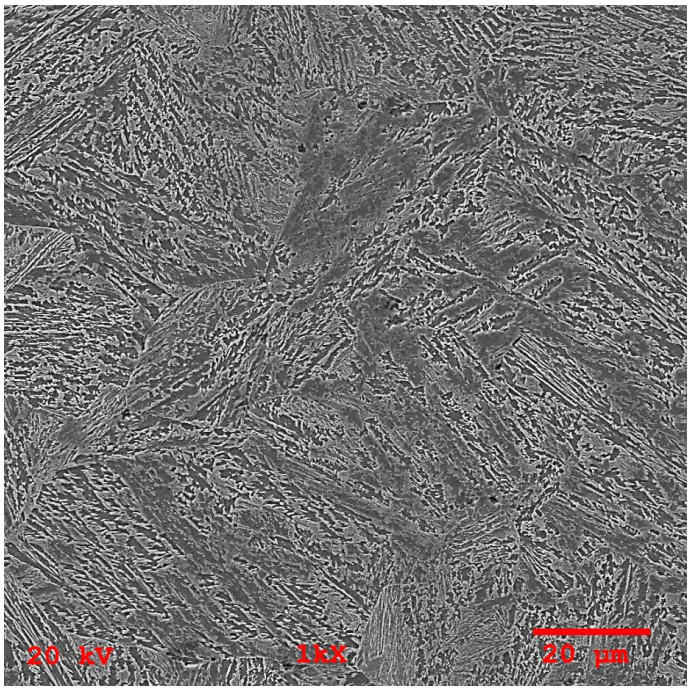

a.

*Figure 4-11 SEM micrographs of G1 after hot forging and continuous cooling **a.** 1000x magnification **b.** 3000x magnification **c.** 5000x magnification*

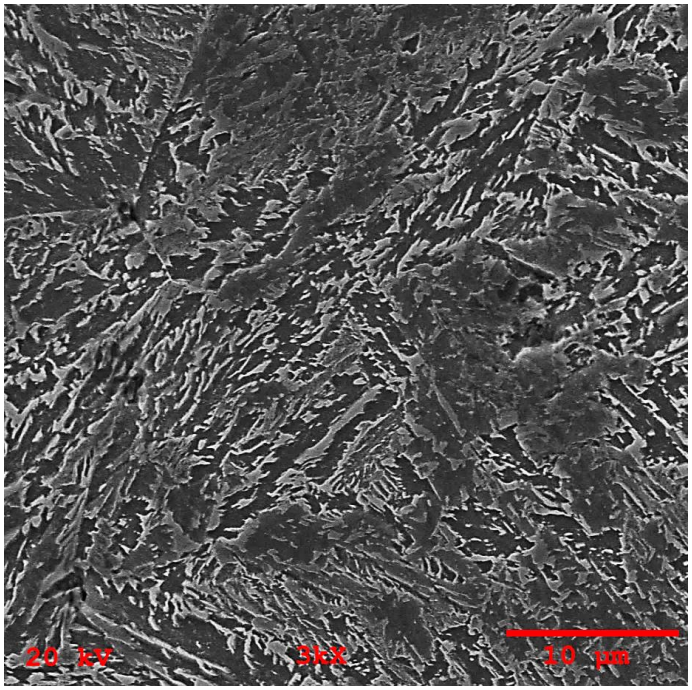

b.

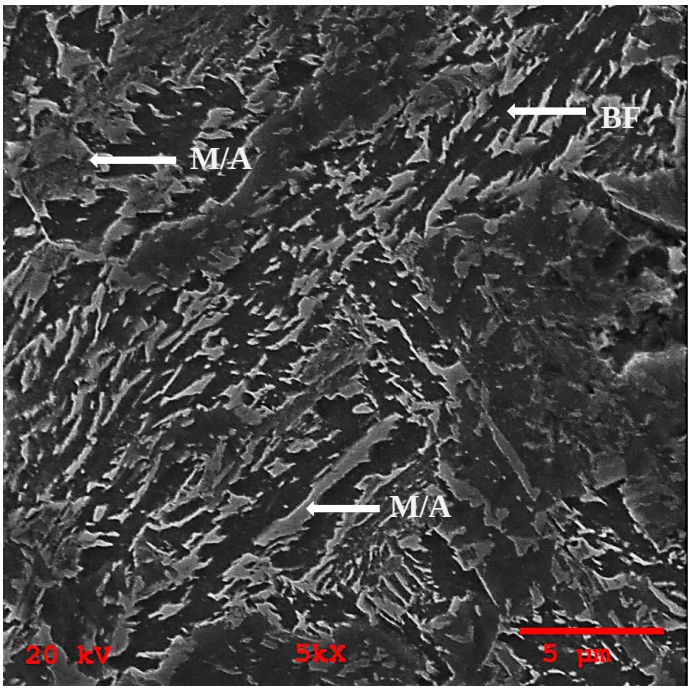

c.

Figure 4-11 (continued)

In **Figure 4-12,** G4 steel grade is investigated. At higher magnifications blocky and flat type retained austenite phases are clearly seen and shown as M/A. Blocky and flat type M/A phases are seen as islands and they may transform to martensite upon cooling to room temperature. Carbides are not encountered in microstructure because of the high silicon content of steel (1.40%), so only bainitic ferrite phase is present. The microstructure is similar to previous grades. In this specimen, the bainite sheaves seems to be more thinner than the previous specimens.

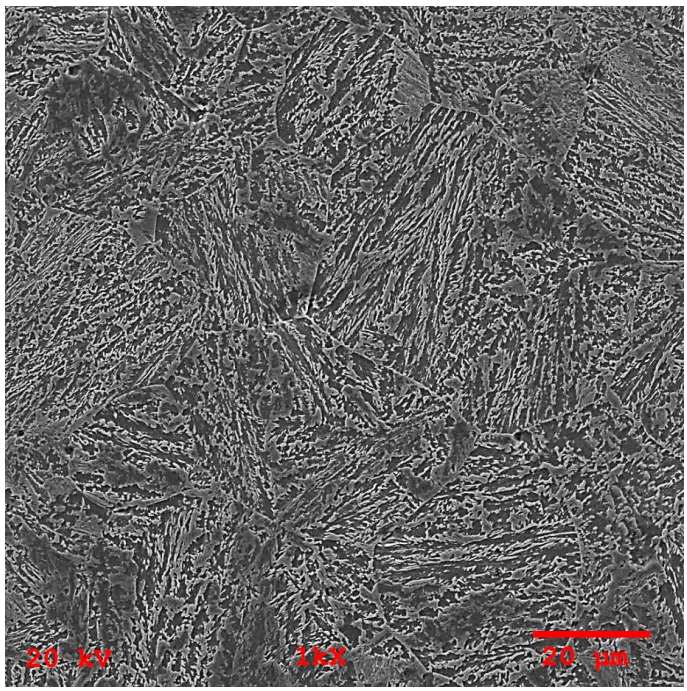

a.

*Figure 4-12 SEM micrographs of G4 after hot forging and continuous cooling **a.** 1000x magnification **b.** 3000x magnification **c.** 5000x magnification*

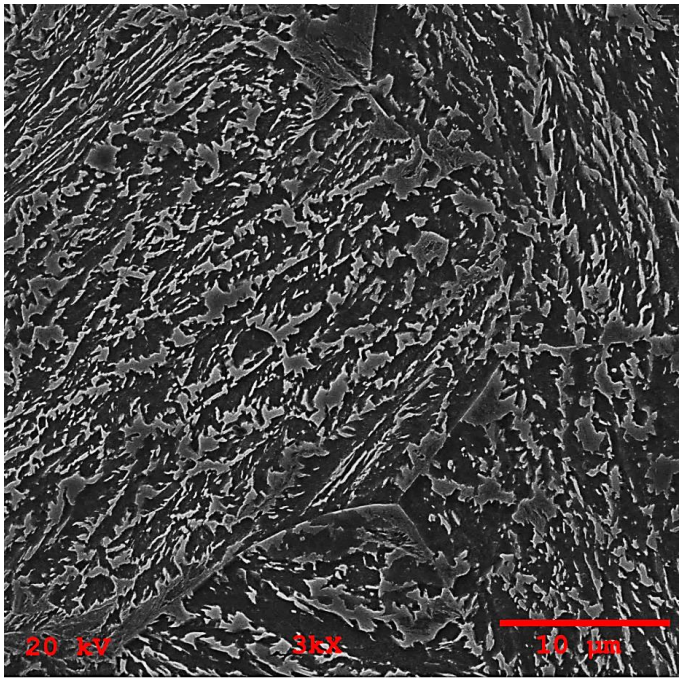

b.

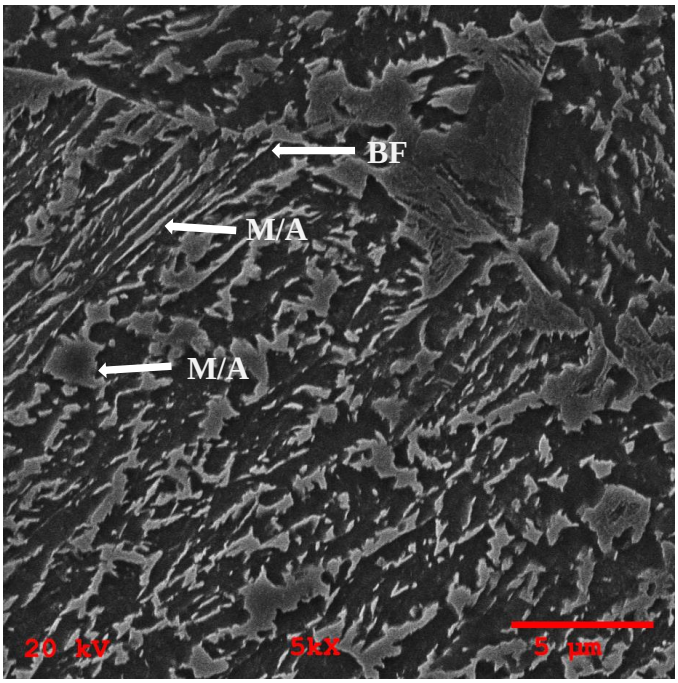

c.

Figure 4-12 (continued)

In **Figure 4-13,** G5 steel grade is investigated. At higher magnifications blocky and flat type retained austenite phases are clearly seen and shown as M/A. Blocky and flat type M/A phases are seen as islands and they may transform to martensite upon cooling to room temperature. Carbides are not encountered in microstructure because of the high silicon content of steel (1.40%), so only bainitic ferrite phase is present. In this steel, the amount of blocky M/A islands seems to be higher than other grades.

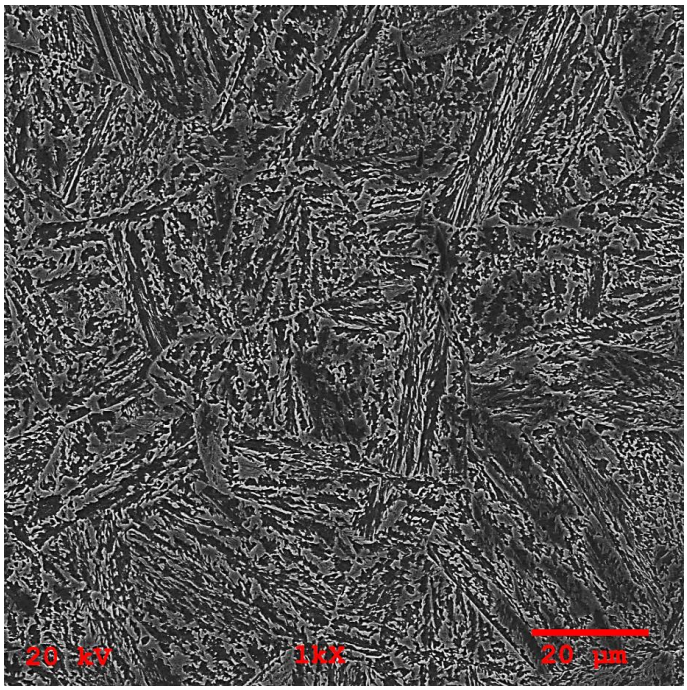

a.

*Figure 4-13 SEM micrographs of G5 after hot forging and continuous cooling **a.** 1000x magnification **b.** 3000x magnification **c.** 5000x magnification*

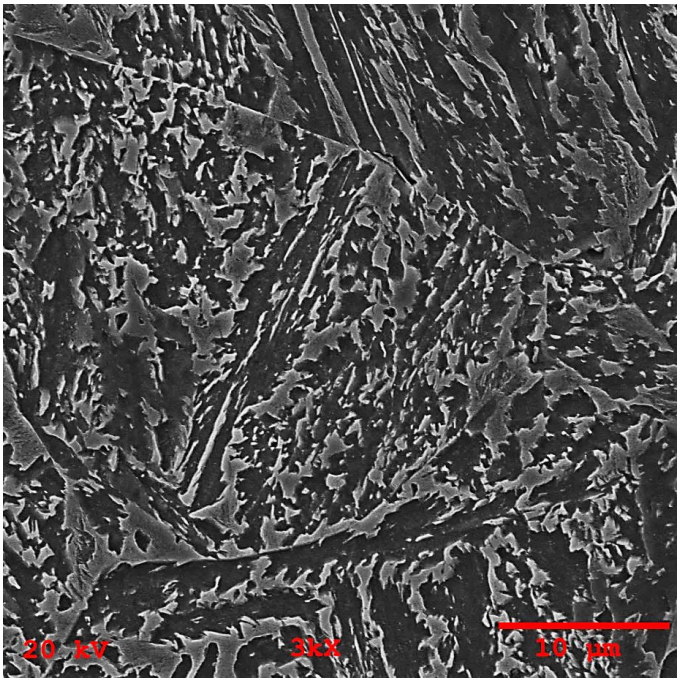

b.

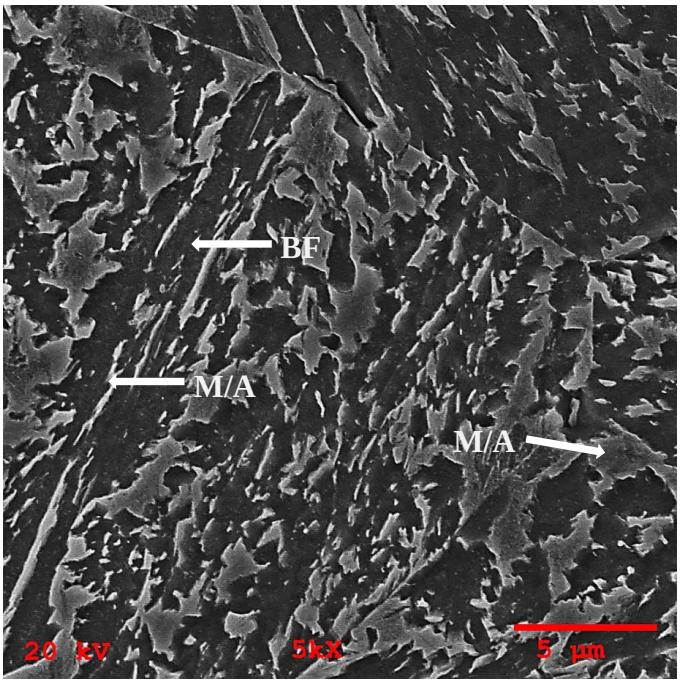

c.

Figure 4-13 (continued)

In **Figure 4-14,** G6 steel grade is investigated. At higher magnifications blocky and flat type retained austenite phases are clearly seen and shown as M/A. Blocky and flat type M/A phases are seen as islands and they may transform to martensite upon cooling to room temperature. Carbides are not encountered in microstructure because of the high silicon content of steel (1.40%), so only bainitic ferrite phase is present. In this specimen, the bainite sheaves seems to be more thinner than the previous specimens.

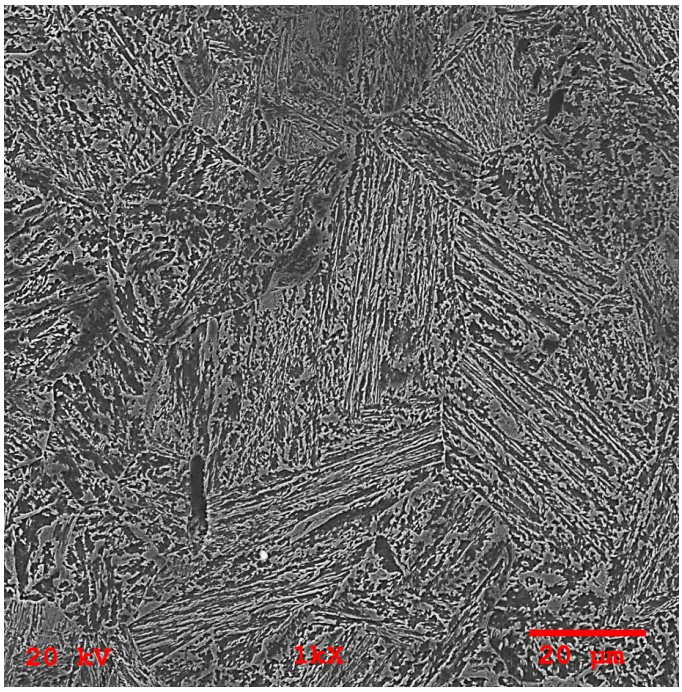

a.

*Figure 4-14 SEM micrographs of G6 after hot forging and continuous cooling **a.** 1000x magnification **b.** 3000x magnification **c.** 5000x magnification*

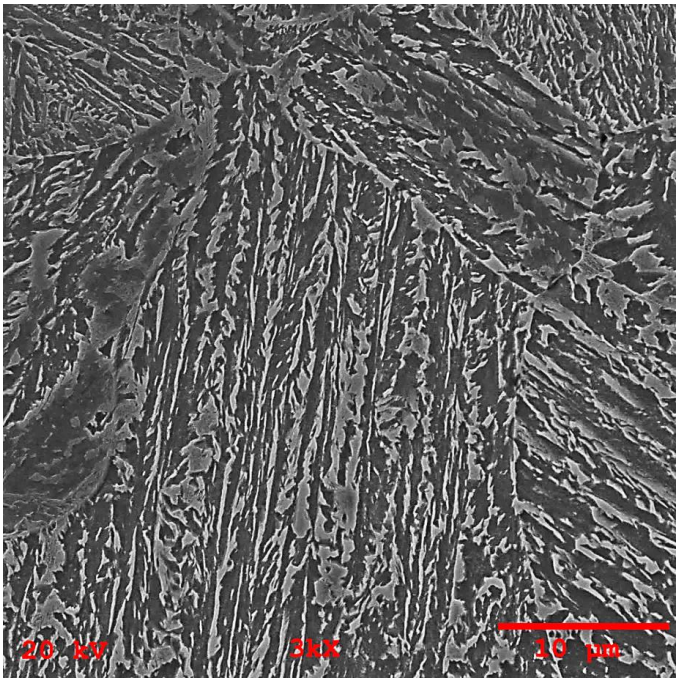

b.

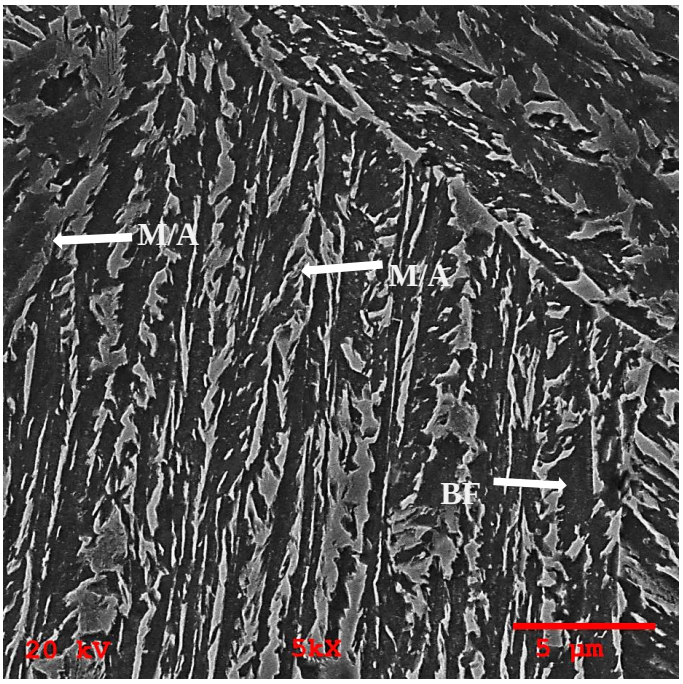

c.

Figure 4-14 (continued)

Bainite thicknesses were calculated for each grade from SEM pictures as it is seen in **Figure 4-15**. Thickness values are obtained from 6 different parts of steel. Results are shown in **Table 4-1**.

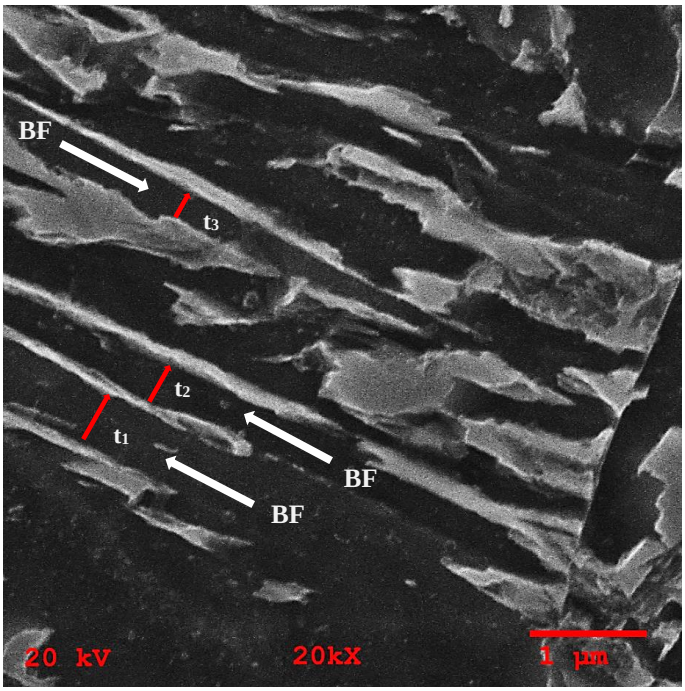

Figure 4-15 Bainitic ferrite between flat type of M/A phase under SEM, 20000x magnification

Table 4-1 Bainite thickness results

Steel Grade	t_1(µm)	t_2(µm)	t_3(µm)	t_4(µm)	t_5(µm)	t_6(µm)	Ave. (µm)
Ref. Steel Grade	0.58	0.54	0.78	0.64	0.59	0.61	0.62±0,08
G1	0.65	0.74	0.59	0.68	0.66	0.78	0.68±0,07
G4	0.81	0.68	0.67	0.71	0.77	0.66	0.72±0,06
G5	0.72	0.72	0.70	0.84	0.82	0.55	0.73±0,10
G6	0.62	0.72	0.68	0.72	0.64	0.68	0.68±0,04

Results show that bainite thickness of reference steel grade is less than other experimental steel grades. Bainite thickness of new steel grades are close to each other. Since, thickness of bainite can be related with UTS better strength is expected for reference steel grade.

4.2.3. Austenite grain size results

Austenite grain size was measured according to ASTM E-112. The results are close and they are shown in **Figure 4-16**. G5 has the highest niobium and titanium, but its grain size is not the finest. In addition, G4 has the lowest content of titanium and niobium and it has finer grains than G5. Thus, their austenite grain size cannot be discriminated with this level of variation in Ti and Nb content.

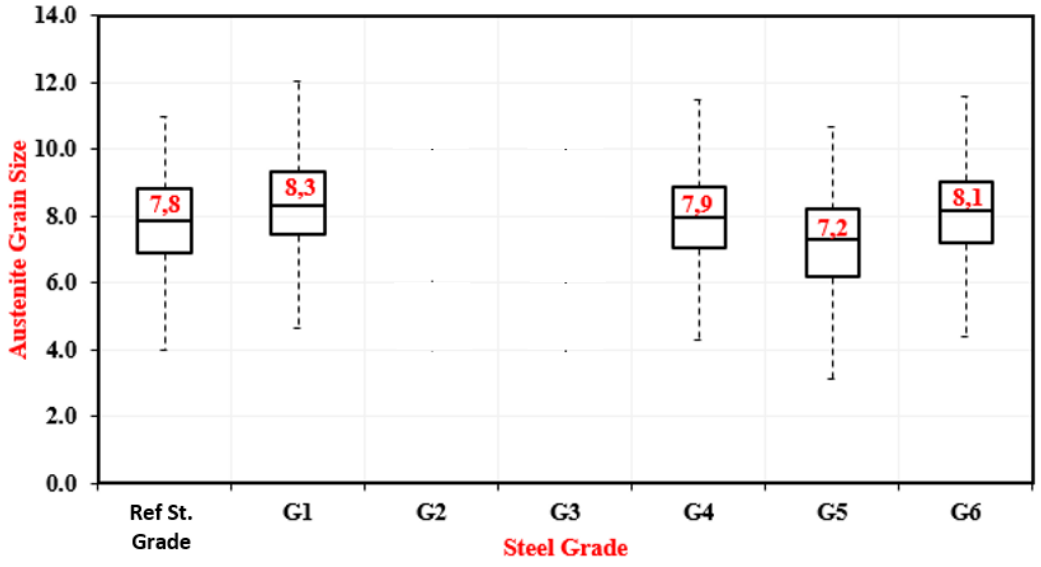

Figure 4-16 Austenite grain size of each steel grade according to ASTM E-112

4.3. Mechanical Properties

As it is seen in **Figure 4-17** yield strength of G4 is measured 772 Mpa. All new steel grades have higher yield strength value than reference steel grade.

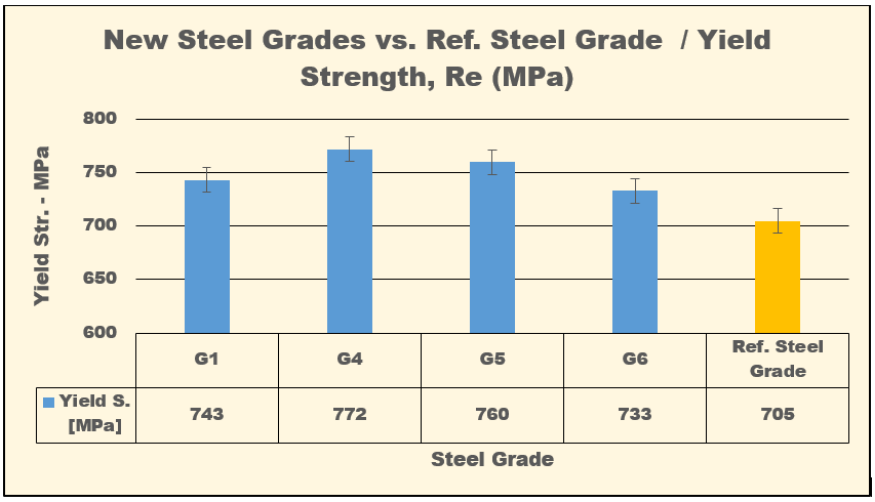

Figure 4-17 Yield strength comparison of each steel grade

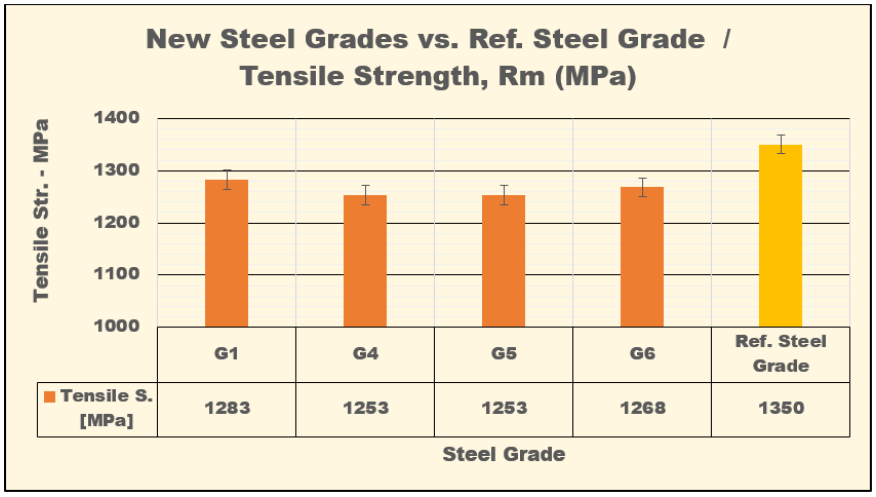

Figure 4-18 Tensile strength comparison of each steel grade

In **Figure 4-18** tensile strength of new steel grades are less than reference steel. G1 is measured as 1283 MPa that is the highest value of new steel grades.

When new steel grades are compared with reference steel grade, their elongation is higher than others except G6 **(Figure 4-19)**. G1 elongates 16,2%.

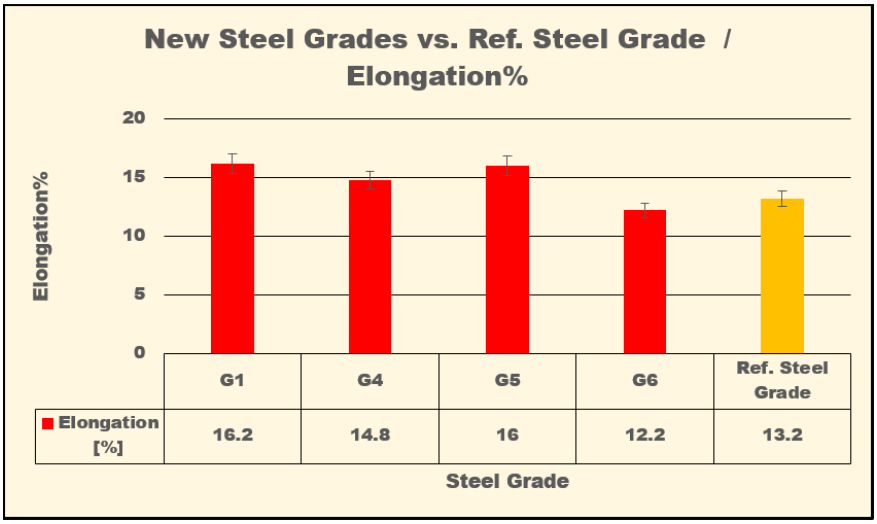

Figure 4-19 Elongation percent comparison of each steel grade

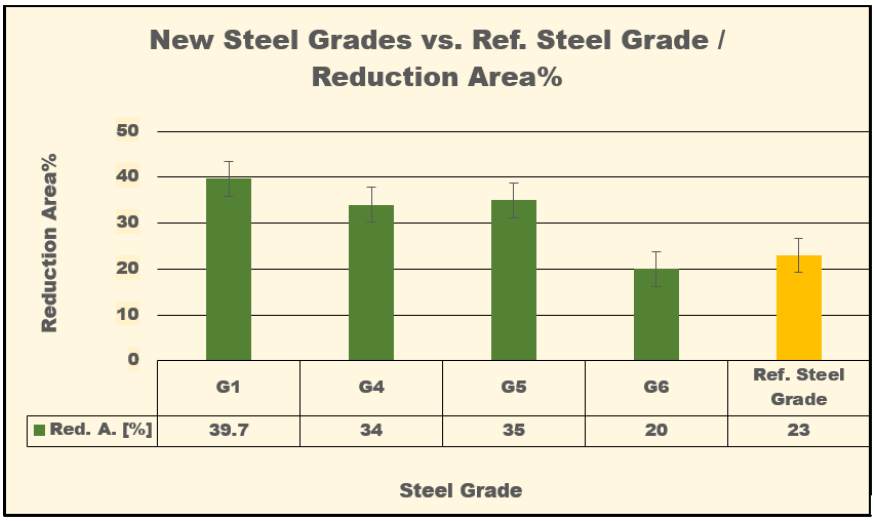

Figure 4-20 Reduction area percent comparison of each steel grade

Area reduction is measured and it is shown in **Figure 4-20**. G1, G4 and G5 have higher percentages than reference steel grade.

In **Figure 4-21**, measured toughness values are seen. New grades have higher toughness values.

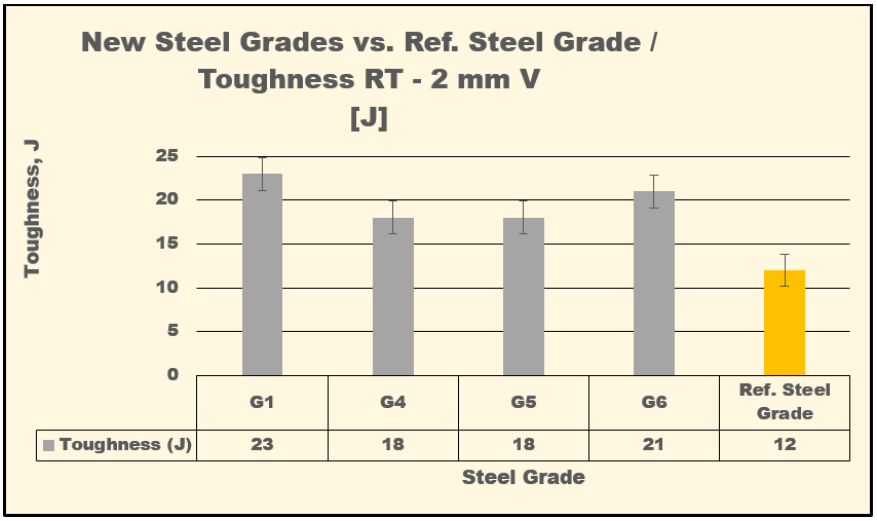

Figure 4-21 Toughness comparison of each steel grade

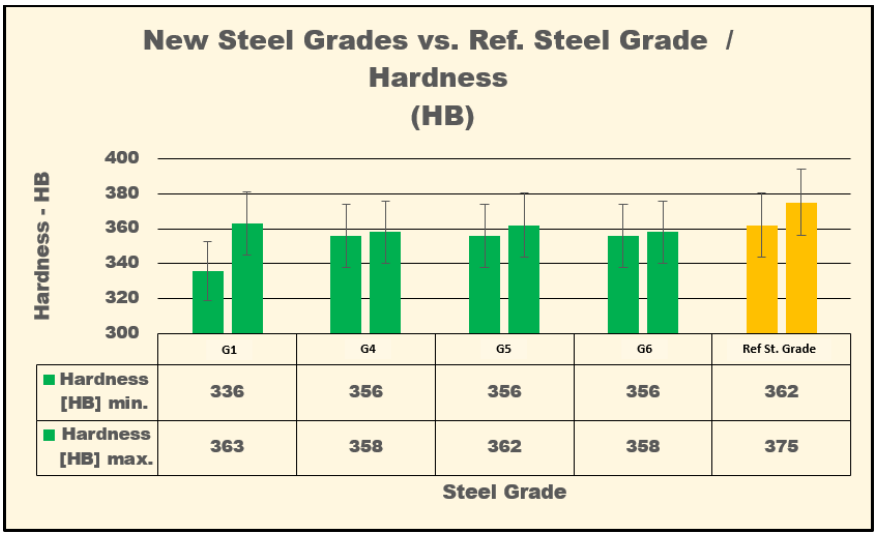

Figure 4-22 Hardness comparison of each steel grade

Hardness values are compared in **Figure 4-22**. Measured values are close with each other.

The tensile strength of all G series are lower. However, in terms of elongation, the G series steels are performed better than reference steel. Tensile ductility of all steel grades are calculated from combination of **Figure 4-18** and **Figure 4-19**. The results are given **Table 4-2**.

Table 4-2 Tensile ductility comparison of each grade

Steel Grade	**Tensile Ductility (UTS x %Elongation)**
Reference Steel	17.8 GPa
G1	20.8 GPa
G4	18.6 GPa
G5	20.0 GPa
G6	15.5 GPa

It is seen that G series (except G6) exhibit better strength-ductility balance when they are compared with reference steel grade. They are capable of sustaining large plastic deformations at high strength levels.

4.4. Dilatometer Results

As it is seen from **Figure 4-16,** austenite grain size of G series are close to each other. Moreover, it can be said that close mechanical properties are obtained and they cannot be discriminated with their titanium or niobium content. Thus, G4 represents the G-series in comparison with reference steel grade for dilatometer testing.

Samples are heated up to 1200ºC and dimensional change is calculated upon cooling by dilatometer. Argon is used to arrange temperature decrease during test.

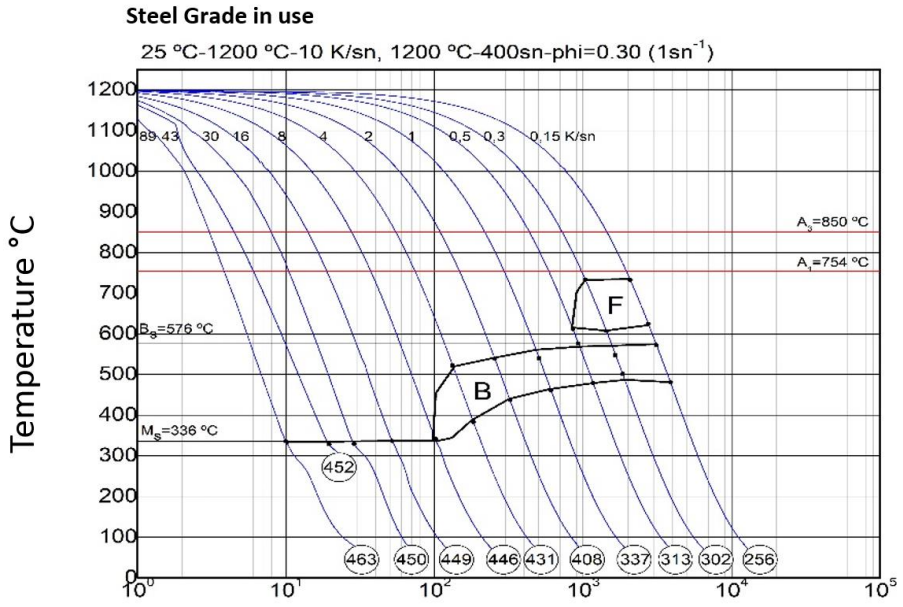

Figure 4-23 Precise CCT diagram of reference steel grade with hardness values in different cooling rates

After dilatometer testing, precise CCT diagram of reference steel grade is drawn. As it is seen from **Figure 4-23**, a cooling rate between 8K/sec and 0.5K/sec yields highest amount of bainite. Hardness values obtained for all cooling rates are also given on the graph as HV. Hardness value decreases by decreasing cooling rate of the steel.

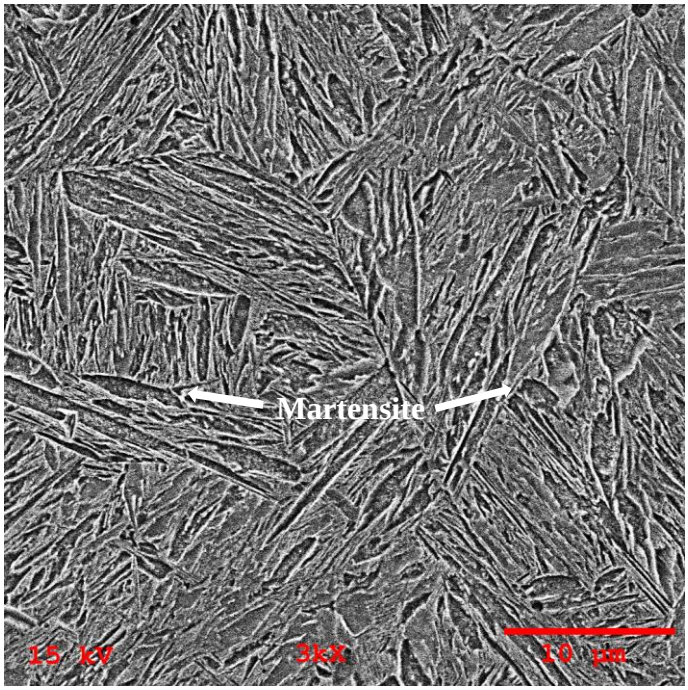

a.

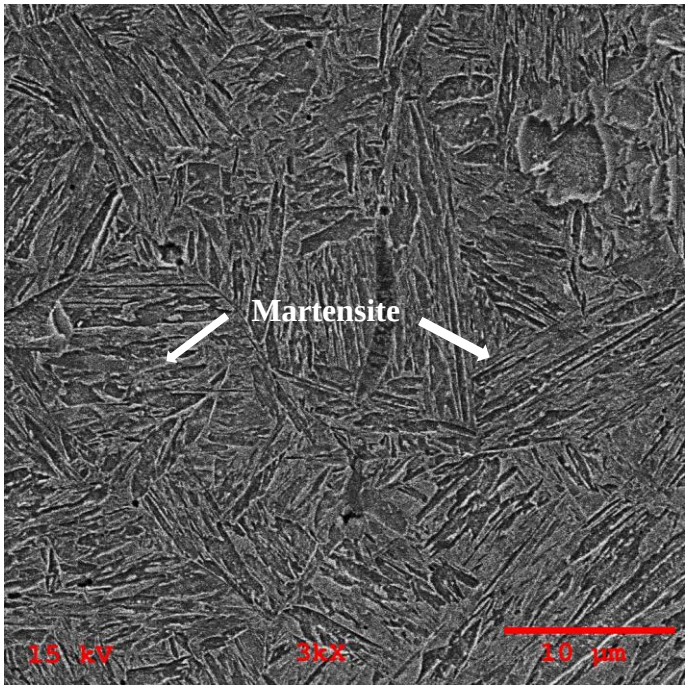

b.

Figure 4-24 Microstructure images of reference steel grade with different cooling rates ***a.****42K/sec* ***b.****30K/sec* ***c.****16K/sec* ***d.****8K/sec* ***e.****2K/sec* ***f.****1K/sec* ***g.****0,5K/sec* ***h.****0,3K/sec* ***i.****0,15K/sec*

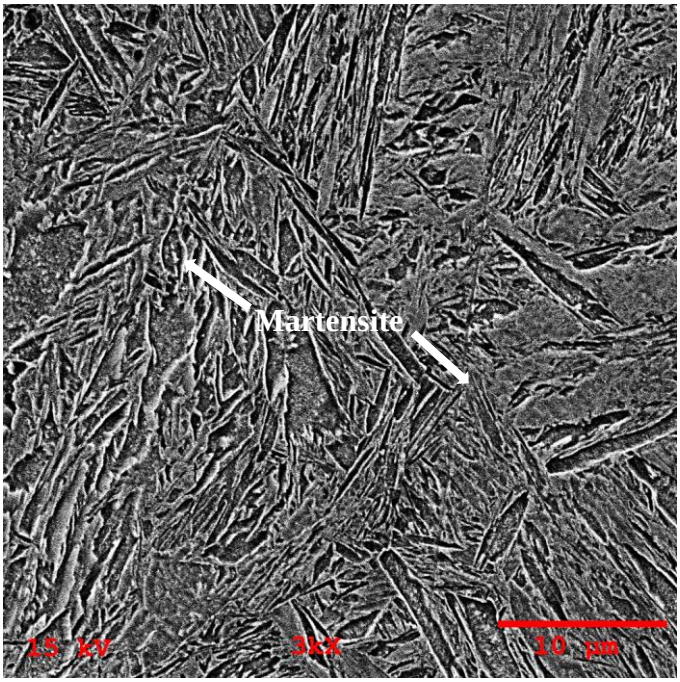

c.

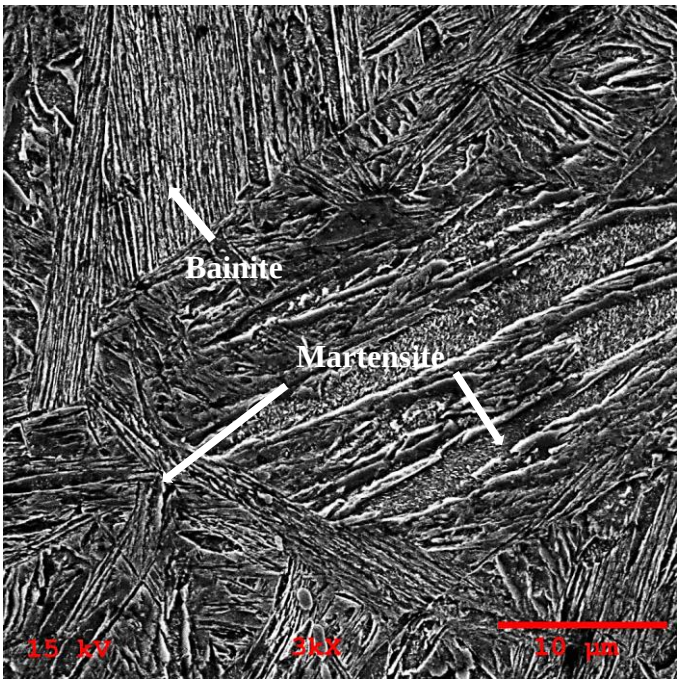

d.

Figure 4-24 (continued)

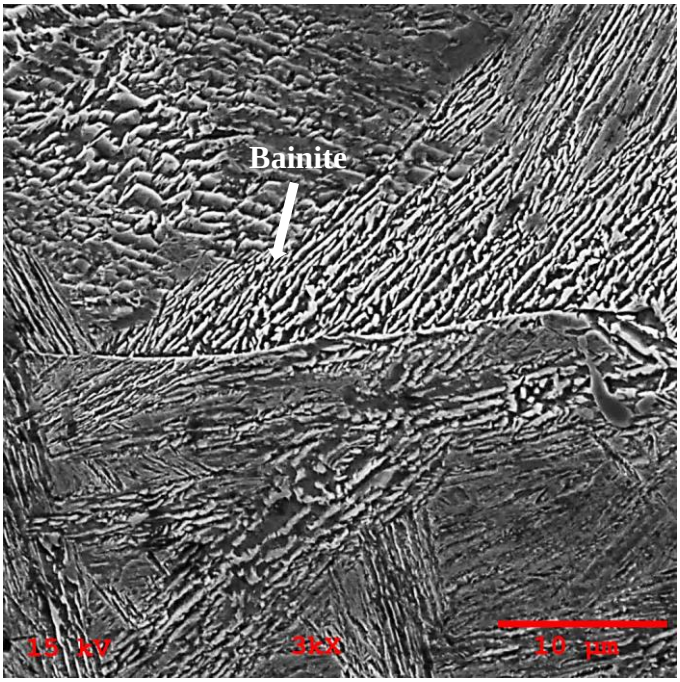

e.

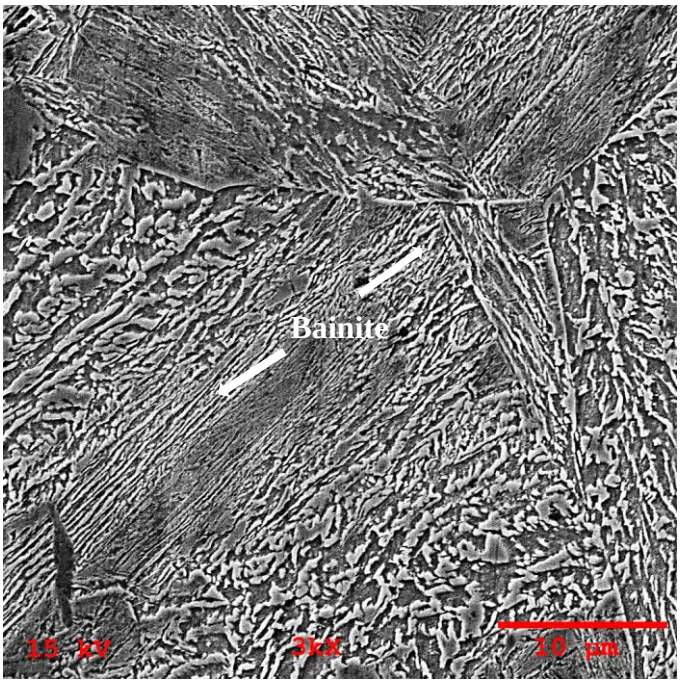

f.

Figure 4-24 (continued)

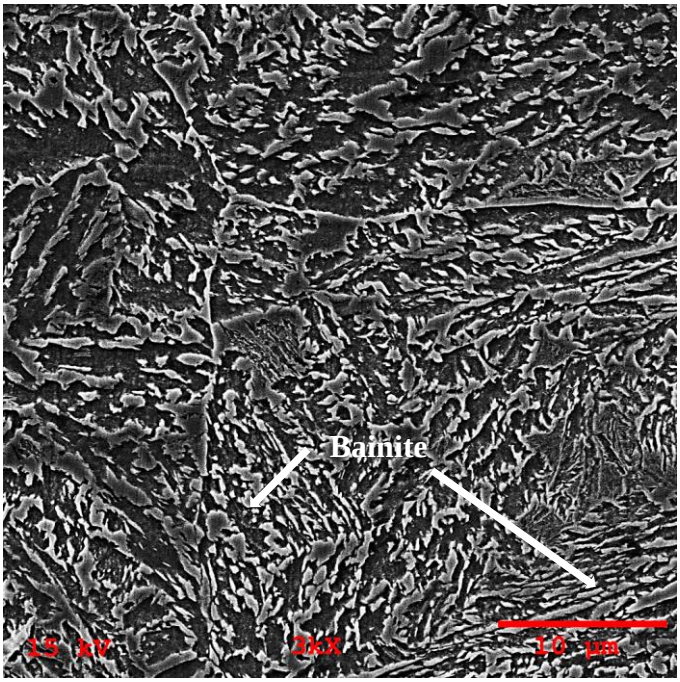

g.

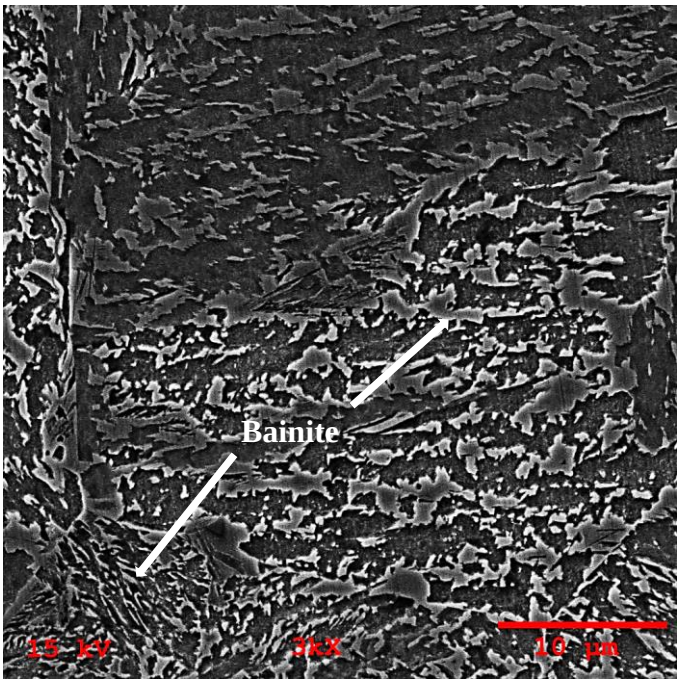

h.

Figure 4-24 (continued)

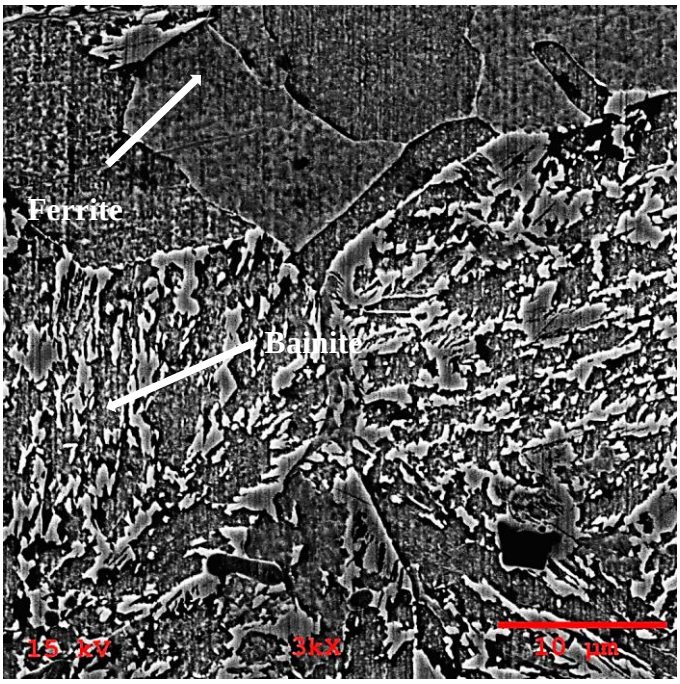

i.

Figure 4-24 (continued)

Dilatometer samples of reference steel grade are heated up to 1200^{o}C. In **Figure 4-24**, microstructure images of reference steel grade are seen with different cooling rates after dilatometer testing. Cooling rate of 2-3K/sec, which is working parameter after hot forging process bainite forms. Between 42K/sec and 16K/sec martensite is clearly seen. After 8K/sec, bainite starts to form it presents with martensite. After 0.3K/sec proeutectoid ferrite starts to form and in picture of specimen **(i)**, which is cooled by 0.15K/sec, proeutectoid ferrite can be clearly seen.

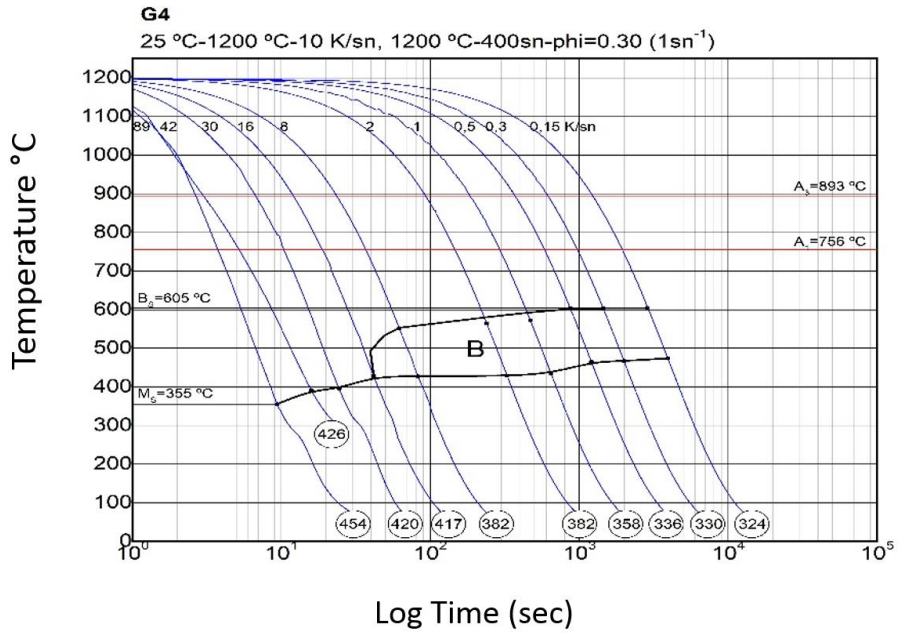

Figure 4-25 Precise CCT diagram of G4 with hardness values in different cooling rates

In **Figure 4-25**, precise CCT graph of G4 steel grade can be seen after dilatometer testing. As seen, a cooling rate between 16K/sec and 0.15K/sec yields highest amount of bainite. Hardness values obtained for all cooling rates are also given on the graph as HV. Hardness value decreases by decreasing cooling rate of the steel.

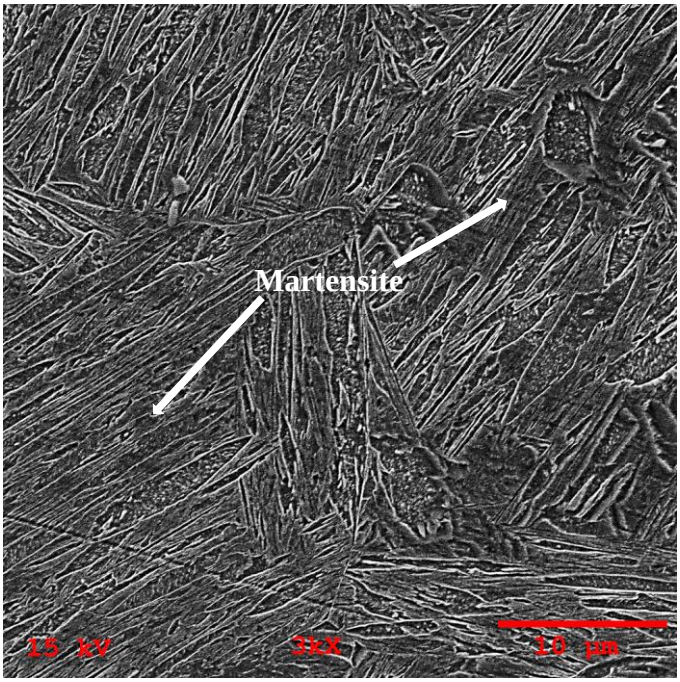

a.

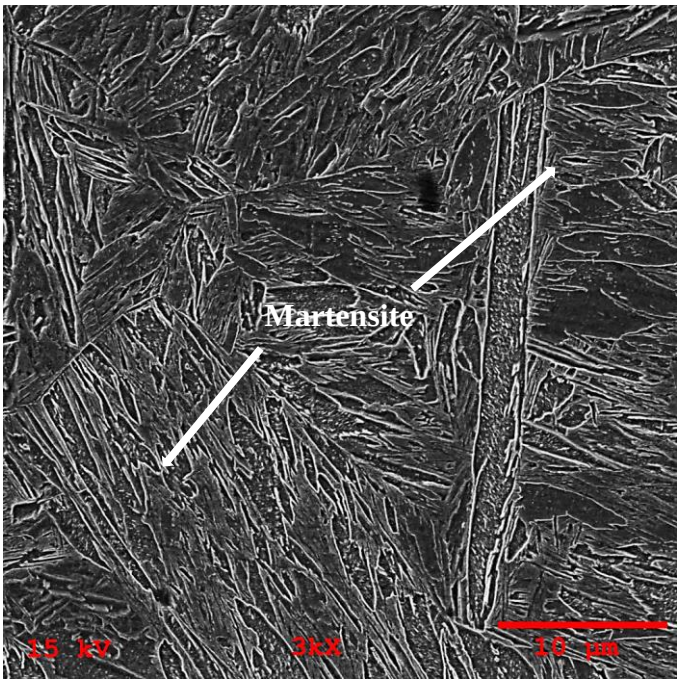

b.

Figure 4-26 Microstructure images of G4 with different cooling rates ***a.*** *42K/sec* ***b.*** *30K/sec* ***c.****16K/sec* ***d.****8K/sec* ***e.****2K/sec* ***f.****1K/sec* ***g.****0,5K/sec* ***h.****0,3K/sec* ***i.****0,15K/sec*

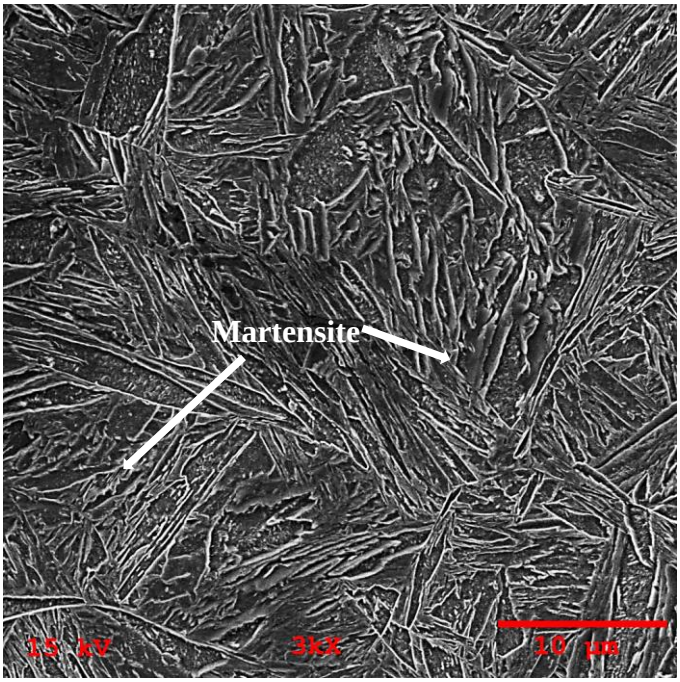

c.

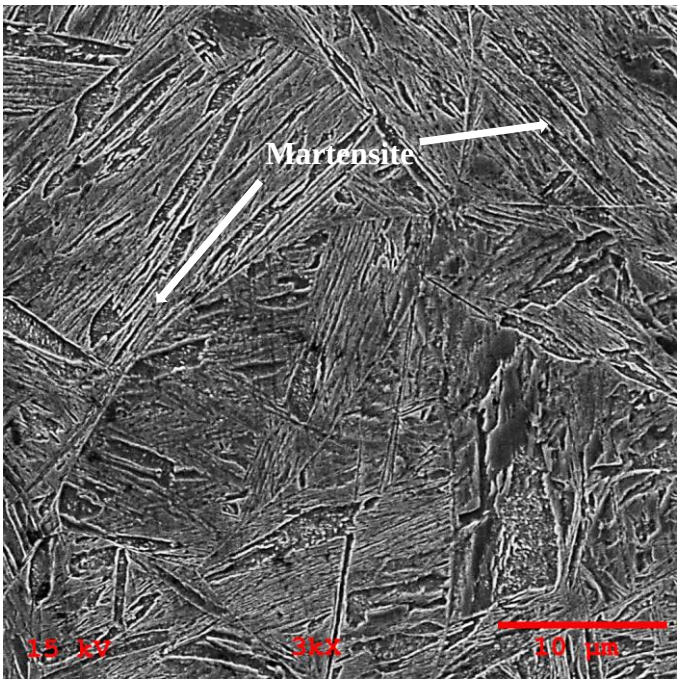

d.

Figure 4-26 (continued)

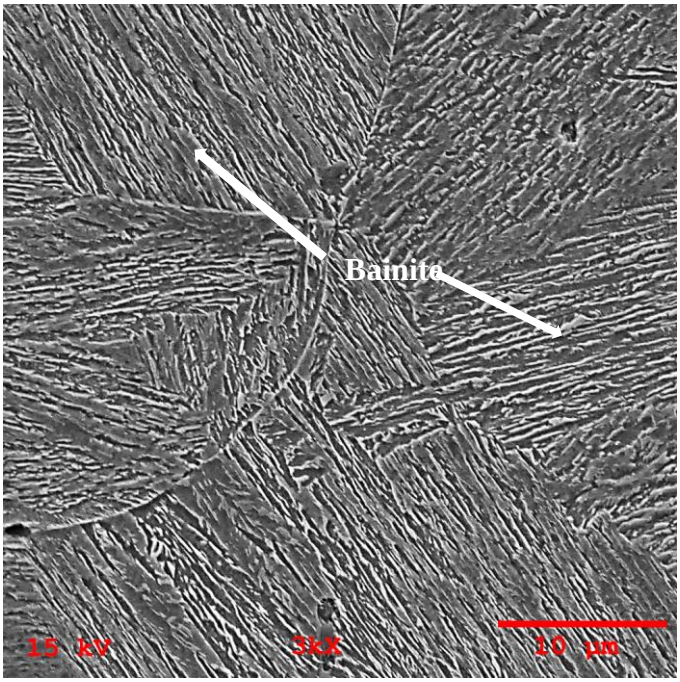

e.

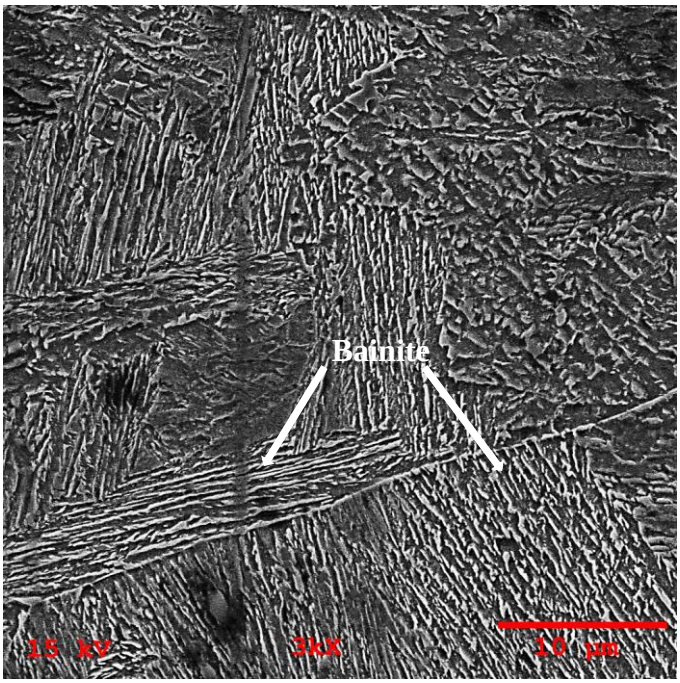

f.

Figure 4-26 (continued)

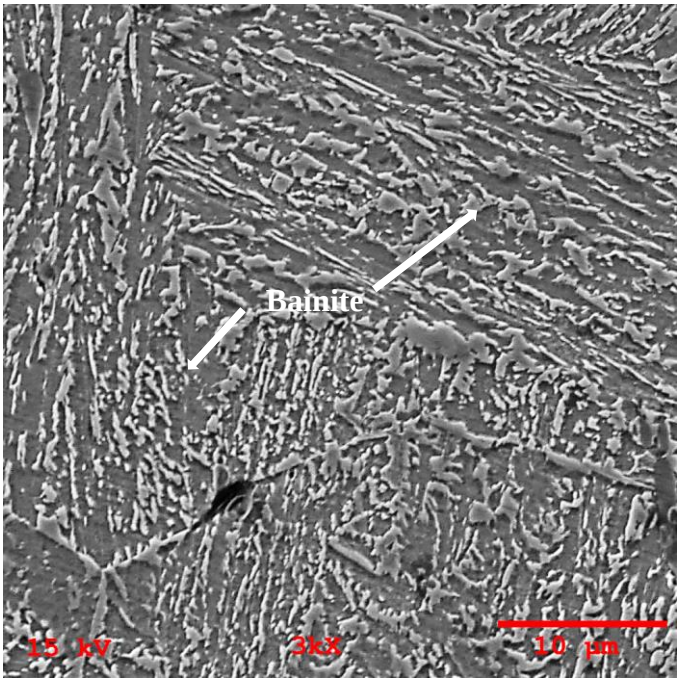

g.

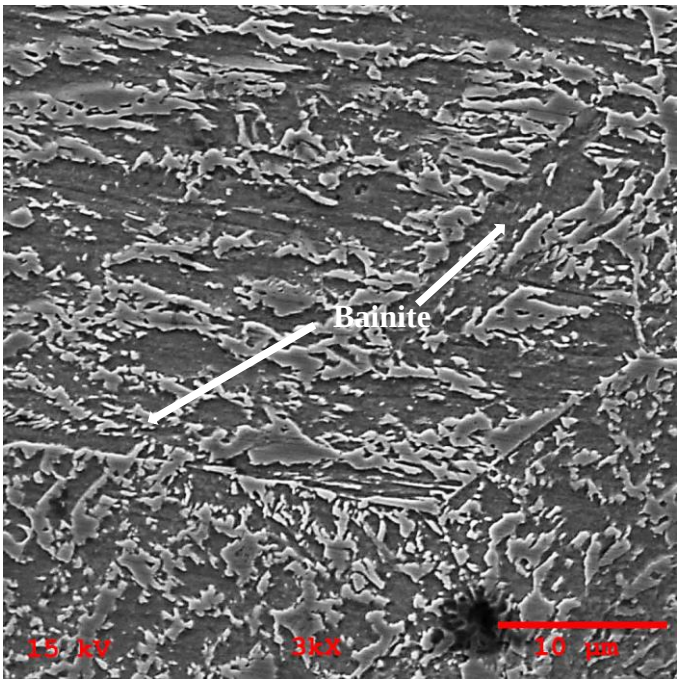

h.

Figure 4-26 (continued)

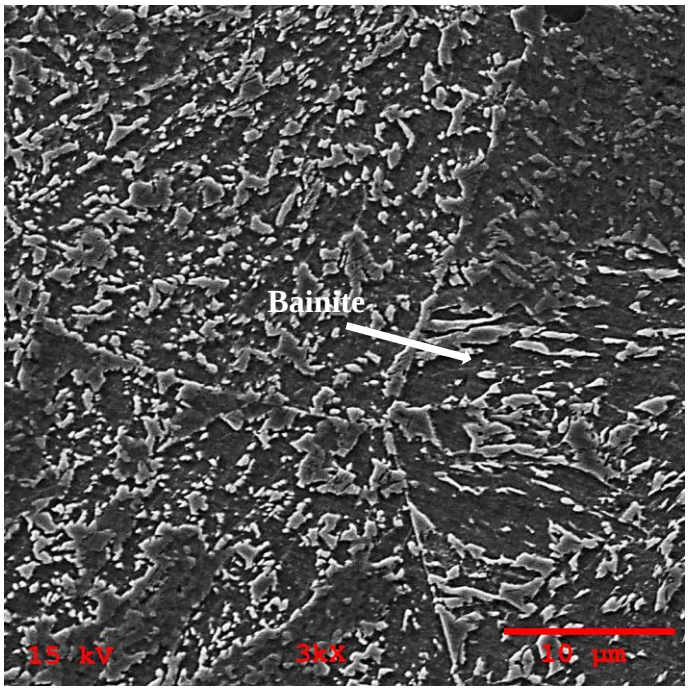

i.

Figure 4-26 (continued)

Dilatometer samples of G4 are heated up to 1200^{o}C. In **Figure 4-26**, SEM images of G4 is seen in different cooling rates. When it is compared with reference steel grade bainite starts to form after 16K/sec. Bainite sheaves present until 0.3K/sec. When it is cooled slower coarser bainite microstructure is seen and bainitic ferrite thickness is increasing. However, there is no proeutectoid ferrite formation like in reference steel grade at slow cooling rates.

4.5. XRD Results

From **Figure 4-27** to **Figure 4-31**, XRD patterns of G1, G4, G5, G6 and reference steel grade are shown. The results obtained show that α-iron and γ-iron present in microstructure and there is no carbide.

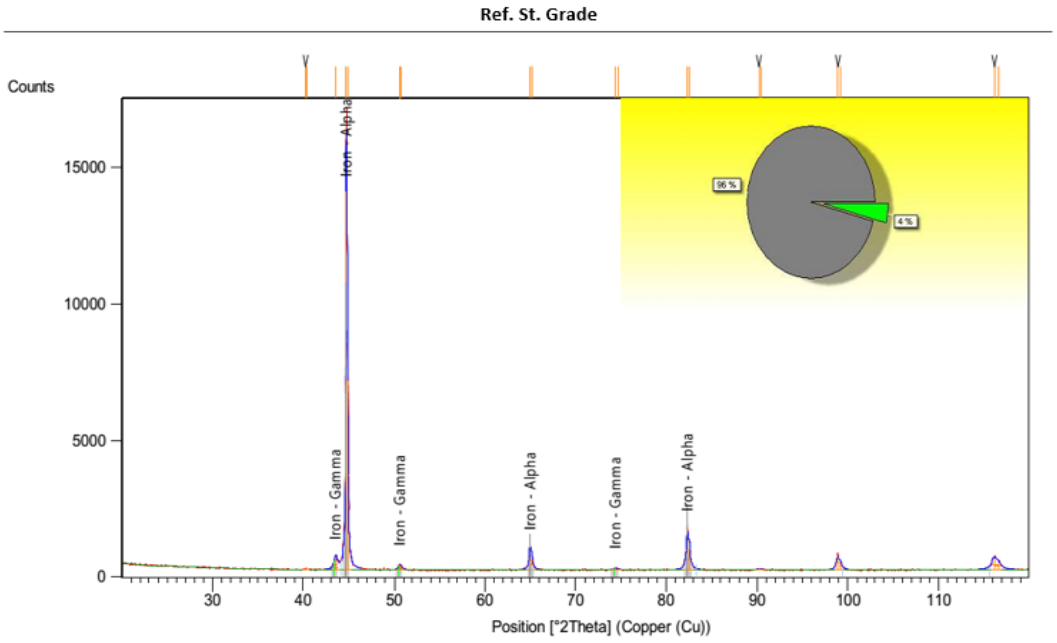

Figure 4-27 Diffraction angles of Reference Steel Grade by using Cu-K α radiation

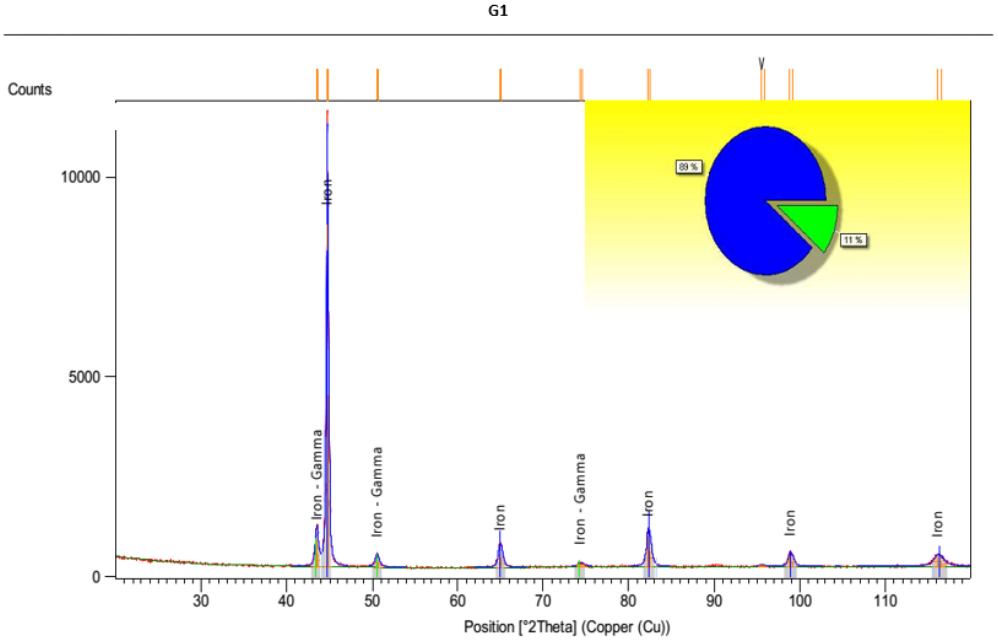

Figure 4-28 Diffraction angles of G1 by using Cu-K α radiation

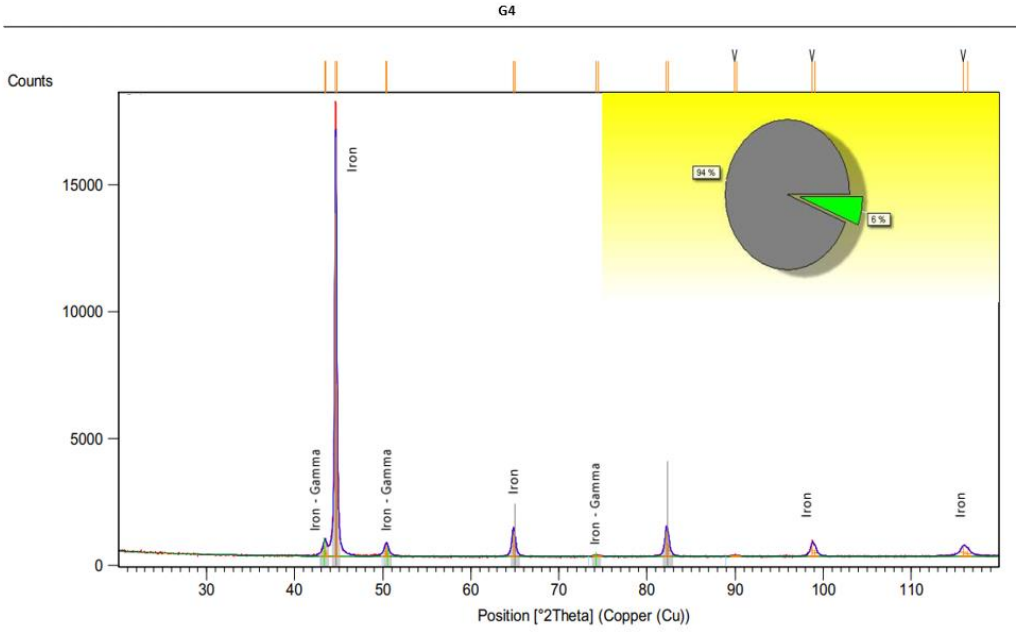

Figure 4-29 Diffraction angles of G4 by using Cu-K α radiation

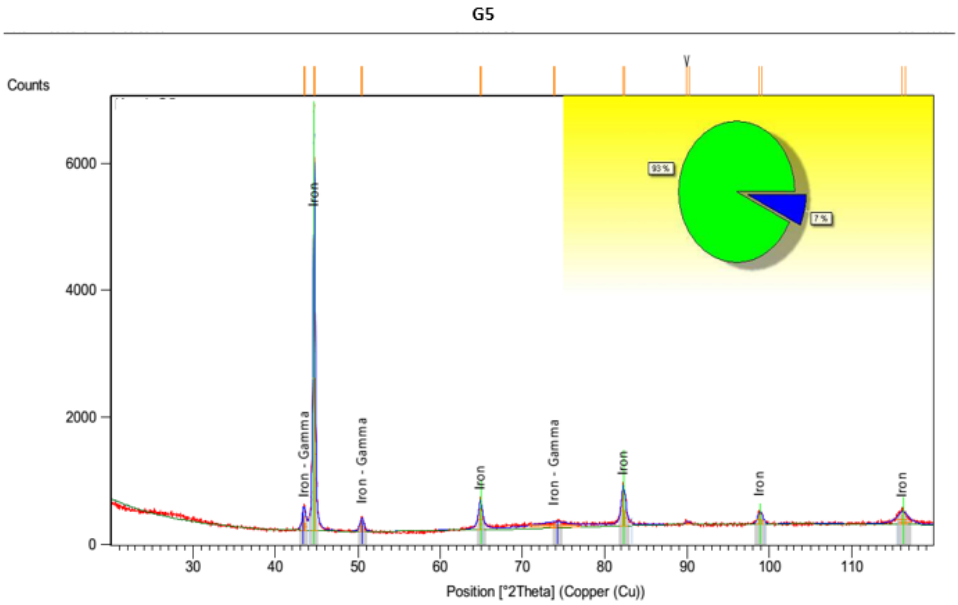

Figure 4-30 Diffraction angles of G5 by using Cu-K α radiation

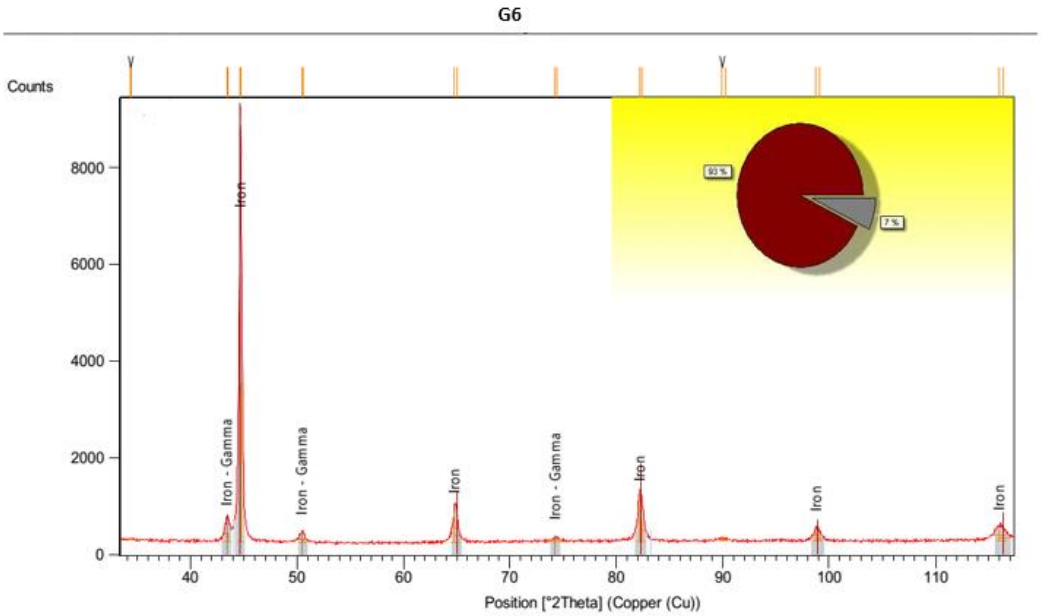

Figure 4-31 Diffraction angles of G6 by using Cu-K α radiation

To calculate volume fraction of retained austenite the formula given below is used.

$$Vi = 1/(1 + \mathrm{G}(\mathrm{I}\alpha/\mathrm{I}\gamma))$$

Where V_i is the volume fraction of austenite for each peak, I_α and I_γ are the corresponding integrated densities of ferrite/bainite and austenite, and the G value is chosen as follows, 2.5 for $I_\alpha(200)/I_\gamma(200)$, 1,38 for $I_\alpha(200)/I_\gamma(220)$, 1.19 for $I_\alpha(211)/I_\gamma(200)$ and 0.06 for $I_\alpha(211)/I_\gamma(220)$[50]. Volume fraction of retained austenite of each grades are given **Table 4-3**.

Table 4-3 Volume fraction of retained austenite of each grade

Steel Grade	**Volume fraction of retained austenite**
Reference Steel	0.04
G1	0.11
G4	0.06
G5	0.07
G6	0.07

CHAPTER 5

DISCUSSION

5.1. Alloying elements

G1 is the base composition at the beginning of this study. It is designed in the view of the recent literature search and using Jmatpro CCT simulations. First, a high percentage of silicon is added in order to suppress the carbide precipitation in bainite. When there is no carbide precipitation, the bainitic ferrite sheaves reject the carbon to austenite. This causes saturation of austenite with respect to carbon and austenite retention upon cooling to room temperature. As the blocky retained austenite islands are very similar to that of martensite, they are named as M/A. It is aimed that the retained austenite together with bainite sheaves help to improve both the strength and ductility.

Since carbon content is lowered, total chromium and molybdenum content is increased to shift CCT diagram right and retard formation of pearlite/ferrite structure in continuous cooling and also to enhance the mechanical properties in terms of solid solution strengthening.

Boron is also used in design of similar alloys. It is known that boron retards ferrite and pearlite formation even if it is added in small amounts. Titanium is needed for boron added steels, because it has higher affinity with nitrogen than boron. Therefore, boron can stay in solid solution whereas titanium bonds nitrogen atoms as TiN.

Aluminum is used less than reference steel grade in new steel grades. Aluminum can be used to obtain finer grain size. However, it contaminates steel with inclusions and has negative effect on mechanical properties. It is known that, Al also suppress carbide formation, however, silicon is used for that purpose in this study.

G2 and G3 are designed for a better machinability, as an increase in sulphur causes an increase in the amount of MnS inclusions, which are known to improve the machinability.

G1, G4, G5 and G6 are designed with different amount of titanium and niobium additions. They are used as micro-alloying elements and it is known that they have a strong effect in grain refinement.

5.2. Mechanical Properties

G1, G4, G5, G6 and reference steel grade are investigated. The main difference between reference steel grade and G series are in toughness, elongation and reduction area percentages. G series show better or similar yield strength values than reference steel. However, the tensile strength of all G series are lower. In terms of elongation and toughness, again the G series steels are performed better than reference steel. Especially, the higher toughness values of the G series steels can be related to the higher amount of retained austenite, since the retained austenite volume fraction of new steel grades are found higher than reference steel grade (XRD results). As it is mentioned, retained austenite in bainitic steel enhance primarily toughness and elongation properties.

UTS value is higher for the reference steel grade. It can be associated with bainitic ferrite thicknesses. Since, the thicknesses of bainitic sheaves of reference steel grade is lower than G series alloys, the higher strength of the reference steel can be related to finer bainitic structure.

G1, G4, G5 and G6 contain only different amount of titanium and niobium. It can be said that close mechanical properties are obtained and they cannot be discriminated with their titanium or niobium content. G5 has the highest niobium and titanium, but their mechanical properties are not different than others. In addition, G4 has the lowest content of titanium and niobium and it has the highest yield strength value. Therefore, the effect of titanium and niobium on mechanical properties is not prior consideration during selection of alloy with these contents.

5.3. Metallographic examinations

New steel grades of G series and reference steel grade are all have bainitic microstructure upon cooling 2-3K/sec. They are investigated under both optical and scanning electron microscope. Bainitic ferrites are clearly seen and between ferrites mixed type of morphology of retained austenite and martensite which is called in literature as M/A. No carbides are seen in G series, which supports the claim that silicon suppressed the formation of carbides.

Since mechanical properties of G1, G4, G5 and G6 are close to each other; TiN contents of steels are considered. TiN inclusions have sharp corners and they have a stress concentration effect, which may cause cracks and less energy absorption. G4 and G6 has the lowest amount of titanium. Thus, their TiN distribution in steel is lowered and failure risk is decreased.

5.4. CCT diagrams

CCT diagrams are simulated during alloy design. After dilatometer tests, the precise diagrams of G4 and reference steel are obtained. It is seen that, bainite can form at a larger interval of cooling rate. It is seen that the pearlite/ferrite formation is retarded due to addition of chromium and molybdenum. As a result, critical cooling rate is raised up to 16K/sec for bainite formation in G4, though this value is only 8K/sec for reference steel grade. Moreover, it is seen that proeutectoid ferrite formation starts at higher cooling rates in reference steel grade, which may cause dramatic decrease of strength.

5.5. X-Ray Diffraction

G-series have higher amount of retained austenite phase in their microstructure when they are compared with the reference steel grade. It is known that retained austenite phase enhance mechanical properties especially elongation and toughness. It is shown that %elongation, %reduction area and toughness of G-series are higher with respect to reference steel. By increasing the Si content of G series steels, carbide precipitation

is suppressed and probably higher amount of carbon is rejected to austenite phase and hence higher amount of austenite is stabilized. It is known that a silicon content of 1.5% or higher is effective in prevention of carbide precipitation in carbide free bainite [51]. G1 has the highest volume fraction of retained austenite between new alloys.

CHAPTER 6

CONCLUSION

In this experiment, a new bainitic steel alloy is designed for hot forged diesel engine parts. The effect of Si, Ti, Nb and S on bainite formation and mechanical properties are studied.

1. In all experimental compositions, i.e. G series steels, carbide free bainite could be obtained. In addition, the microstructure contain retained austenite phase in the range 6%-11%.

2. The tensile strength of the experimental steels are at around 1270MPa and meet the 1100 MPa criteria.

3. As far as the % elongation and toughness of the experimental steels are concerned, G series steels are performed better than their commercial counterpart by yielding an elongation of around 16% and charpy impact toughness values in the range 18J-23J. The higher toughness of the G series steels are attributed to their lower carbon and higher amount of retained austenite contents.

4. The dilatometer test results have shown that in experimental steel G4 (0.01%Ti added), the bainite formation is possible at a large interval of cooling rate which can be an advantage in industrial forging practice.

5.As far as the cost is taken into consideration together with mechanical properties, the experimental steel 0.2C-1.50Si-1.40Mn-1.45(Cr+Mo) with 0.01%Ti addition can be a good candidate for a continuous cooled bainitic forging steel.

REFERENCES

[1]- S. Engineer, P. Janssen, M. Härtel, C. Hampel and F. Randelhoff: 'Technological properties of the new high-strength bainitic steel 20MnCrMo7', Proc. 3rd Int. Conf. on '*Steels in cars and trucks*', Salzburg, 2011, 404–411.

[2]- C. Keul, V. Wirths, W. Bleck, New bainitic steels for forgings, *archives of civil and mechanical engineering 12* (2 0 1 2) 119–125.

[3]- B. Buchmayr, Critical Assessment 22: Bainitic forging steels, *Materials Science and Technology*, (2016), 32:6, 517-522.

[4]- Bhadeshia H.K.D.H, *Bainite in The Steel-Transformations, Microstructure and Properties,* 3nd ed., University of Cambridge,UK, 2006.

[5]- Sherif M.Y., Characterisation and Development of Nanostructured, Ultrahigh Strength, and Ductile Bainitic Steels, Doctoral Thesis, University of Cambridge, Department of Materials Science and Metallurgy, Cambridge, 2006.

[6]- M. Takahashi and H. K. D. H. Bhadeshia. Transition from upper to lower bainite. Mat. Sci. Tech., 6:592, 1990.

[7]- Krauss G., *Steels: Processing, Structure, and Performance*, 2nd ed., ASM International, Ohio, 2015.

[8]- Podder A.S. Tempering of a Mixture of Bainite and Retained Austenite, Doctoral Thesis, University of Cambridge, Department of Materials Science and Metallurgy, Cambridge, 2011.

[9]- Bhadeshia H.K.D.H, *Bainite in Steels,* 2nd ed. University of Cambridge,UK, Cambridge, 2001.

[10]- Hillert M., Diffusion in Growth of Bainite, *Metallurgical and Material Transactions A.*, 1994, 25a,1957-1965.

[11]- Hillert M., Paradigm Shift for Bainite, *Scripta Materialia*, 2002, 47, 175-180

[12]- Bramfitt B.L., Speer J.G., A Perspective on the Morphology of Bainite, *Metallurgical and Material Transactions A.*, 1990, 21a, S. 817-829.

[13]- Joarder A., On the Bainite Structure in Cr-Mo-V Rotor Steel, *Steel Research Nr. 8*, 1994, 65, 345-349.

[14]- Bhadeshia H.K.D.H., Edmonds D.V., The Bainite Transformation in a Silicon Steel, *Metallurgical Transactions A*, 1979, 10a, 895-907.

[15]- Jacques P.J., Furnémont Q., Pardoen T., Delannay Q.F., On the Role of Martensitic Transformation on Damage and Cracking Resistance in TRIPAssisted Multiphase Steels, *Acta Materialia*, 2001, 49, 139-152.

[16]- Hilditch B.T.; Timokhina I.B.; Robertson L.T.; Pereloma E.V.; Hodgson P.D., Cyclic Deformation of Advanced High-Strength Steels: Mechanical Behavior and Microstructural Analysis, *Metallurgical and Materials Transactions A*, 2009, 49A, 342-353.

[17]- Cheng X., Petrov R., Zhao L., Janssen M., Fatigue Crack Growth in TRIP Steel Under Positive R-Ratios, *Engineering Fracture Mechanics*, 2008, 75, 739-749.

[18]- Tomitaa Y., Iwamoto T., Computational Prediction of Deformation Behavior of TRIP Steels Under Cyclic Loading, *International Journal of Mechanical Sciences*, 2001, 43, 2017-2034.

[19]- Li Z., Fu R., Li Q., Effects of Retained Austenite Stability on Mechanical Properties of High Strength TRIP Steel, *Advanced Materials Research*, 2013, 602-604 , 287-293.

[20]- Zhang S., Findley K.O., Quantitative Assessment of the Effects of Microstructure on the Stability of Retained Austenite in TRIP Steels, *Acta Materialia*, 2013, 61, 1895-1903.

[21]- Edmonds D.V., Advanced Bainitic and Martensitic Steels with Carbide-Free Microstructures Containing Retained Austenite, *Material Science Forum*, 2010, 638-642, 110-117.

[22]- Rees G.I., Bhadeshia H.K.D.H., Bainite Transformation Kinetics Part 1 Modified Model, *Materials Science and Technology*, 1992, 8, 985-993.

[23]- Lawrynowicz Z., Carbon Partitioning During Bainite Transformation in Low Alloy Steels, *Materials Science and Technology Nr. 11*, 2002, 18, 1322-1324.

[24]- Park K.K., Oh S.T., Baeck S.M., Kim D.I., Han J.H., Han H.N., Park S.H., Lee C.G., Kim S.J., Oh K.H., In-situ Deformation Behavior of Retained Austenite on TRIP Steel, *Material Science Forum*, 2002, 408-412, 571-576.

[25]- Timokhina I.B., Hodgson P.D., Pereloma E.V., Effect of Microstructure on the Stability of Retained Austenite in Transfomation-Induced-Plasticity Steels, *Metallurgical and Materials Transactions A*, 2004, 35A, 2331-2341.

[26]- Suikkanen P., Development and Processing of Low Carbon Bainitic Steel, Doctoral Thesis, Universitatis Ouluensis, Faculty of Technology PohjoisPohjanmaa, 2009.

[27]- Campbell F.C., *Elements of Metallurgy and Engineering Alloys*, 1st ed., ASM International,Ohio, 2008.

[28]- Campbell F.C., Phase Diagrams-Understanding the Basics, 1st ed., ASM International, Ohio, 303-338, 2012.

[29]- Garcia-Mateo C., Caballero F.G., Role of Retained Austenite on Tensile Properties of Steels with Bainitic Microstructures, *Materials Transactions Nr. 8*, 2005, 46, 1839-1846.

[30]- Bhadeshia H.K.D.H, High Performance Bainitic Steels, *Materials Science Forum, ,* 2005, 500-501, 63-74.

[31]- Jacques P.J., Girault E., Catlin T., Geerlofs N., Kop T., Zwaag S. van der, Delannay F., Bainite Transformation of Low Carbon Mn-Si TRIP-Assisted Multiphase Steels: Influence of Silicon Content on Cementite Precipitation and Austenite Retention, *Materials Science and Engineering A,* 1999, 273-275, 475-479.

[32]- Keh A.S., Leslie W.C., Recent Observations on Quench-Aging and Strain Aging of Iron and Steel, *Materials Science Research,* 1963, 1, 208-250.

[33]- Traint S., Pichler A., Heuzberger K., Stiazny P., Werner E., Influence of Silicon, Aluminum, Phosphorus and Copper on the Phase Transformations of Low Alloy TRIP-Steels, *Steel research Nr. 6+7,* 2002, 73, 259-266.

[34]- Kozeschnik, E., & Bhadeshia, H. (2008). Influence of silicon on cementite precipitation in steels, *Material Science and Technology,* 24(3), 343-348.

[35]- Quidort D., Brechet Y., The Role of Carbon on the Kinetics of Bainite Transformation in Steels, *Scripta Materialia Nr. 3*, 2002, 47, 151-156.

[36]- Reynolds W.T.Jr., Shui C.K., Aaronson H.I., The Incomplete t-Transformation Phenomenon in Fe-C-Mo Alloys, *Metallurgical Transactions Nr. 6*, 1990, 21, 1433-1462.

[37]- Taş Z., Yüksek Dayanımlı Düşük Alaşımlı Çeliklerde Metalurjik Mukavemet Artırma Mekanizmaları, *Erciyes Üniversitesi Fen Bilimleri Enstitüsü Dergisi*, 2012, 28(2), 97-101.

[38]- Lienert T., Siewert T., Babu S., Acoff V., *ASM Handbook, Volume 6A: Welding Fundamentals and Processes*, 1st ed., ASM International, Ohio, 2011.

[39]- Zhu K., Oberbillig C., Musik C., Loison D., Iung T., Effect of B and B + Nb on the Bainitic Transformation in Low Carbon Steels, *Materials Science and Engineering A Nr. 12*, 2011, 528, 4222-4231.

[40]- Hanzaki A.Z., Hodgson P.D., Yue S., The Influence of Bainite on Retained Austenite Characteristics in Si-Mn TRIP Steels, *ISIJ International Nr. 1*, 1995, 35, 79-85.

[41]- Kammouni A., Saikalya S., Dumont M., Marteau C., Bano X., Charaï A., Effect of the Bainitic Transformation Temperature on Retained Austenite Fraction and Stability in Ti Microalloyed TRIP Steels, *Materials Science and Engineering Nr. 1+2*, 2008, 518, 89-96.

[42]- Diaz-Fuentes M., Gutiérrez I., Analysis of Different Acicular Ferrite Microstructures Generated in a Medium-Carbon Molybdenum Steel, *Materials Science and Engineering Nr. 1+2*, 2003, 363, 316-324.

[43]- Zhang X., Xu G., Wang X., Embury D., Bouaziz O., Purdy G.R., Zurob H.S., Mechanical Behavior of Carbide-free Medium Carbon Bainitic Steels, *Metallurgical and Materials Transactions A Nr. 3*, 2014, 45, 1352-1361.

[44]- Biablobrzeska B., Konat L., Jasinski R., The Influence of Austenite Grain Size on the Mechanical Properties of Low-Alloy Steel with Boron, *Metals 2017*, 7(1), 26.

[45]- Buchmayr *B.*, Critical Assessment 22: Bainitic Forging Steels, *Materials Science and Technology*, 2016, 32:6, 517-522.

[46]- Wirths V., WagenerR., Bleck W., Melz T., Bainitic Forging Steels for Cyclic Loading, *Advanced Materials Research*, 2014, 922, 813-818.

[47]- Wirths V., Bleck W., Bainitic Forging Steels, *29. Aachener Stahlkolloquium*, Aachen, Almanya, 27-28 Mart 2014.

[48]- Balart M.J., Davis C.L., Stangwood M., Fracture Behaviour in MediumCarbon Ti-V-N and V-N Microalloyed Ferritic-Pearlitic and Bainitic Forging Steels with Enhanced Machinability, *Materials Science and Engineering*, 2002, A328, 48-57.

[49]- Eggbauer G., Buchmayr B., High-Strength Bainitic Steels for Forged Products, *BHM Berg- und Hüttenmännische Monatshefter*, 2015, 160(5), 209-213.

[50]- Zhou M., Xu G., Tian J., Bainitic Transformation and Properties of Low Carbon Carbide-Free Bainitic Steels with Cr addition, *The State Key Laboratory of Refractories and Metallurgy*,2017, 263-267.

[51]- E. Kozeschnik & H. K. D. H. Bhadeshia (2008) Influence of silicon on cementite precipitation in steels, *Materials Science and Technology*, 24:3, 343-347.